Functional Dissection of the Dimerization and Enzymatic Activities of *Escherichia coli* Nitrogen Regulator II and Their Regulation by the PII Protein

Peng Jiang, Mariette R. Atkinson, Chatchawan Srisawat, Quan Sun, and Alexander J. Ninfa*

Department of Biological Chemistry, University of Michigan Medical School, Ann Arbor, Michigan 48109-0606

Received April 10, 2000; Revised Manuscript Received August 14, 2000

ABSTRACT: The dimeric two-component system transmitter protein NRII (NtrB) of *Escherichia coli*, product of *glnL* (*ntrB*), controls transcription of nitrogen-regulated genes by catalyzing the phosphorylation and dephosphorylation of the transcription factor NRI (NtrC). Previous studies showed that the PII signal transduction protein inhibits the kinase activity of NRII and activates its phosphatase activity. We observed that PII greatly stimulated the NRII phosphatase activity under conditions where the cleavage of ATP was prevented, indicating that the phosphatase activity did not result simply from prevention of the antagonistic NRII kinase activity by PII. Rather, PII was an activator of the phosphatase activity. To study this regulation, we examined the dimerization and enzymatic activities of NRII and various polypeptides derived from NRII, and their regulation by PII. Our results were consistent with the hypothesis that NRII consists of three domains: an N-terminal domain found only in NRII proteins and two domains formed by the conserved transmitter module of NRII, the phosphotransferase/phosphatase/dimerization (central) domain and the kinase domain. All three domains were involved in regulating the kinase and phosphatase activities of NRII. The N-terminal domain was involved in intramolecular signal transduction, and controlled access to the NRII active site for the isolated dimeric central domain added in trans. The central domain was responsible for dimerization and the phosphotransferase and phosphatase activities of NRII, but the latter activity was weak in the isolated domain and was not regulated by PII. The C-terminal kinase domain was responsible for the kinase activity. The PII protein appeared to interact with the isolated transmitter module of NRII, and not with the N-terminal domain as previously thought, since PII dramatically increased the stoichiometry of autophosphorylation of the isolated transmitter module. However, the phosphatase activity of the transmitter module of NRII was low even in the presence of PII, suggesting that the N-terminal domain was necessary for the central domain to assume the conformation necessary for potent phosphatase activity. Also, PII significantly reduced the rate of transphosphorylation of the isolated central domain by the isolated kinase domain, suggesting that PII interacts directly with the kinase domain. We hypothesize that the binding of PII to the kinase domain of NRII results in an altered conformation that is transmitted to the central and N-terminal domains; this causes the central domain to assume the conformation with potent phosphatase activity.

The two-component signal transduction systems constitute the largest family of signal transduction systems in prokaryotes, and are also found in lower eukaryotes and plants (reviewed in ref *1*). Forming the core of these systems are two protein modules known as the transmitter and receiver. The transmitter modules bind ATP and phosphorylate themselves (autophosphorylation) on a conserved histidine motif (*2*, *3*). [In a small number of cases, for example, the chemotaxis protein CheA, the site of phosphorylation is outside the transmitter module, mapping within a related histidine motif (*4*).] The autophosphorylated forms of these proteins serve as the phosphodonor for autophosphorylation of the receiver module on a conserved aspartate (*2*, *4*, *5*). Depending on the system, phosphoryl groups may be transferred from this receiver module to a conserved histidine within another domain, and from there to yet another receiver, forming a phospho relay system (*6*). In many systems, a single receiver is present. The phosphorylation state of the receiver module (or final receiver module in systems with a phospho relay arrangement) is used to control associated domains with various activities (e.g., ref *7*) or to control separate proteins or macromolecular complexes. In addition to the reactions described above, some transmitters also display phosphatase activity toward the phosphorylated receiver (*7*), and the receivers themselves display "autophosphatase" activities to various extents (*8*). In such cases, it is not known whether the apparent phosphatase activity of the transmitter module represents a unique activity or results from activation of the autophosphatase activity of the phosphorylated receiver.

Comparison of translated DNA sequences for transmitter modules has permitted the identification of several conserved motifs, known as the H-box, N-box, D-box, F-box, and G-box (for the positions of these motifs in NRII,[1] see Figure 2 below). Certain proteins are known, which contain only the N-, D-, F-, and G-boxes, and these proteins have serine kinase activity (e.g., ref *9*). Furthermore, recent studies of

* To whom correspondence should be addressed. Phone: (734) 763-8065. Fax: (734) 763-4581. E-mail: aninfa@umich.edu.

10.1021/bi000794u CCC: $19.00
Published on Web 10/11/2000

the EnvZ transmitter protein, involved in osmotic control of porin gene expression in *E. coli*, have shown that the N-, D-, F-, and G-boxes form a "kinase domain" of the transmitter module, which contains an ATP-binding site related to that found in HSP90 proteins (*10*, *11*). The structure of the CheA protein from a thermophile exhibits a similar domain and ATP binding site for this portion of CheA (*12*). When disconnected from the rest of the protein, the kinase domain of EnvZ is monomeric (*10*). Mutational analysis of the conserved sites in NRII and other transmitters has been consistent with the hypothesis that the N-, D-, F-, and G-boxes of transmitters are involved in ATP binding and autophosphorylation activities (*13*).

The H-box region of the transmitter module contains the conserved histidine that is the site of autophosphorylation in the largest class of transmitter proteins (*3*). A clue about the structure of this portion of the transmitter comes from the structure of the Spo0B protein of *Bacillus subtilis*, which is not itself a transmitter but part of the phospho relay system involved in the control of sporulation. The phospho-accepting histidine of Spo0B is within an α-helix that, along with an adjacent helix, forms a four-helix bundle in the dimeric Spo0B (*14*). The four-helix bundle is the primary dimerization determinant of Spo0B. A similar four-helix arrangement had been previously observed in proteins (e.g., ref *15*). Although CheA does not have a functional H-box that is phosphorylated in the region where the typical transmitter module contains an H-box, this portion of CheA also forms a helix that is part of a four-helix bundle that mediates dimerization of CheA (*12*). Finally, the structure of the isolated four-helix bundle of EnvZ has recently been determined (*16*). Thus, structural studies of EnvZ, CheA, and Spo0B lead to the hypothesis that the transmitter module consists of two domains, consisting of the four-helix bundle and the kinase domain.

In addition to the well-conserved motifs noted above, many transmitters contain recognizable homology in the region immediately downstream from the H-box, designated the X-box (*17*). Mutations in the X-box have been obtained in NRII and the EnvZ transmitter regulating porin gene expression, which decrease the level of negative regulatory function of these in vivo, presumably by diminishing the phosphatase activity of the transmitter protein (*13*, *17*, *18*). The X-box region maps in the portion of these transmitters that is likely to constitute one of the two helices from each subunit that form the four-helix bundle.

The modularity of transmitter proteins was demonstrated by Inouye and colleagues, who showed that the purified kinase domain of EnvZ could phosphorylate a purified peptide from EnvZ containing the H- and X-motifs (*10*). In these studies, the H−X polypeptide was dimeric, while the kinase domain was monomeric (*10*). Similarly, the phospho-accepting domain of CheA can be phosphorylated by the kinase domain derived from CheA (*19*). Kramer and Weiss showed that the autophosphorylation of the NRII transmitter module was retained when it was provided in three segments containing the H−X motifs, the N-motif, and the D-, F-, and G-motifs (*20*). That is, the NRII kinase domain could be fragmented into two segments with retention of function.

The autophosphorylation of all of the (wild-type) transmitter domains probably occurs exclusively by a transintramolecular mechanism, in which one subunit binds ATP and phosphorylates the other subunit in the dimer. Transphosphorylation of subunits was first shown for EnvZ (*21*). The exclusive use of this mechanism was demonstrated with NRII (*22*). In the latter work, heterodimers were formed from wild-type and mutant proteins, and from different mutant proteins, by treatment of protein mixtures with a low concentration of urea (2.8 M) followed by dialysis. This low concentration of urea converted NRII to monomers, but did not prevent NRII subunits from binding ATP. Upon dialysis of the urea, heterodimers were formed in proportion to the ratio of different subunits in the mixtures, suggesting that the subunits that were tested were sorted into dimers randomly (*22*). The pattern of phosphorylation observed in heterodimers containing two mutant subunits or a wild-type and mutant subunit was only consistent with an obligatory transintramolecular autophosphorylation mechanism.

The highly concerted nature of the interactions between subunits in NRII is illustrated by the asymmetry of NRII autophosphorylation (*23*). The equilibrium constant for the autophosphorylation of the first subunit of the NRII dimer is ∼0.35, while that for the phosphorylation of the second subunit is ∼0.0044. The net effect is that at 1 mM ATP, NRII consists mainly of hemiphosphorylated dimers, unless the ADP generated in the reaction is removed (*23*). Isotope exchange experiments suggested that in hemiphosphorylated NRII dimers, the unphosphorylated histidine site is undergoing rapid phosphorylation by ATP and even more rapid reversal of the autophosphorylation reaction (*23*).

The NRII transmitter indirectly controls transcription from nitrogen-regulated promoters by catalzying the phosphorylation and dephosphorylation of the NRI receiver protein, which is only able to activate transcription when phosphorylated. The NRI∼P phosphatase activity of NRII is greatly stimulated when NRII is complexed to the PII signal transduction protein (*7*). Various lines of evidence suggest that the phosphatase activity of NRII is intrinsic and that the role of PII in this activity is strictly regulatory. (i) PII is not a phosphatase in the absence of NRII. (ii) Mutations in NRII can eliminate the activity. (iii) Mutations in NRII can result in the activity in the absence of PII. (iv) Mutations that decrease the extent of autophosphorylation of NRII result in an increase in the basal phosphatase activity in the absence of PII (*13*, *18*). The binding of PII to NRII also results in the inhibition of the rate of NRII autophosphorylation; thus, PII reciprocally regulates the autophosphorylation and phosphatase activities of NRII (*24*). However, although it decreases the rate of autophosphorylation, PII increases the stoichiometry of NRII autophosphorylation (*23*). This increase in the stoichiometry of NRII autophosphorylation was most noticeable when conditions were such that NRII autophosphorylation characteristically occurred at ≤50% of the available sites in the absence of PII (*23*).

Mutations that affect the ability of NRII to act as negative regulator of *glnALG* expression are easily isolated (*25*). Presumably, these mutations diminish the phosphatase activ-

[1] Abbreviations: PK, pyruvate kinase; PEP, phosphoenolpyruvate; BSA, bovine serum albumin; MBP, maltose-binding protein of *E. coli*; NRII, nitrogen regulator II; NtrB, product of *glnL* (*ntrB*); NRI, nitrogen regulator I; NtrC, product of *glnG* (*ntrC*); NRI-N, N-terminal domain of NRI consisting of amino acid residues 1−118 of NRI; PII, signal transduction protein encoded by the *glnB* gene; GS, glutamine synthetase, product of *glnA*.

Table 1: PCR Primers

polypeptide	sequence
NT110 (ds)[a]	5′-CCGAATTCGGATCCTCATTACTCGAGCGGAGCCATCTCCAGCA-3′
NT125 (ds)	5′-CCGAATTCGGATCCTCATTACTCGAGGGCGTGCTGTAGCTGTT-3′
NT135 (ds)	5′-CCGAATTCGGATCCTCATTACTCGAGGCGCACTAAATCACGGGCA-3′
NT145 (ds)	5′-CCGAATTCGGATCCTCATTACTCGAGAAGCGGATTTTTAATCTCA-3′
NT155 (ds)	5′-CCGAATTCGGATCCTCATTACTCGAGGAGCAGCTGCGCCGCGCCA-3′
NT169 (ds)[b]	5′-GGGATCCGTCGACTCATTATTTGGTATATTCGAGTAGTGATGG-3′
NT189 (ds)[c]	5′-GGGATCCGTCGACTCATTACTGCGGCCCCAACAGACGGTC-3′
NT series (us)	5′-CCCGAATTCATATGGCAACAGGCACGCAGCCC-3′
CT190 (ds)	5′-GGGAATTCGAGCTCTGCGAGCGCACGTTCAAGCACCCAACGG-3′
CT190 (us)	5′-GGAATTCCATATGCTGCCCGGTACGCGCGTTACC-3′
CT151 (us)	5′-GGAATTCCATATGGCGGCGCAGCTGCTCAGCAAA-3′
CT126 (us)	5′-GGAATTCCATATGCAGCAGGTTGCTGCCCGTGAT-3′
CT126 (ds)[d]	5′-CCAAGCTTGAGCTCGCGAGCGCACGTTCAAGCACCCAACGG-3′
HX_3 (us)	5′-GGAATTCCATATGCAGGAACAGCTACAGCACGCC-3′
HX_2 (us)[e]	5′-GGAATTCCATATGATCCTGCTGGAGATGGCT-3′

[a] Upstream and downstream primers are designated us and ds, respectively. [b] This primer was also used as the ds primer for H_1. [c] This primer was also used as the ds primer for HX_2 and HX_3. [d] This primer was also used as the ds primer for CT151. [e] This primer was also used as the us primer for H_1.

ity of NRII. While most of these mutations mapped near the site of autophosphorylation in the H-box region, other mutations mapped to the N-terminal domain of NRII, to the linker connecting the N-terminal domain to the H-box region, and to the X-box region. Kramer and Weiss demonstrated that the phosphatase activity of NRII resides in a short peptide (residues 123−221 of NRII) that contains the H-box and X-box regions (*20*). Overexpression of this polypeptide fused to the N-terminal domain of λ repressor resulted in negative regulation of *glnA* expression in vivo. Also, the purified fusion polypeptide brought about the dephosphorylation of NRI∼P in vitro. Thus, together the genetic and biochemical data suggest that the phosphatase activity resides in the H−X segment, and that a precise conformation of this segment is required, which is affected by distant parts of NRII.

In this paper, we characterize the roles of the domains of NRII in its activities and interaction with the PII protein.

MATERIALS AND METHODS

Purified Proteins. NRII, NRII-H139N, MBP−NRII, MBP−CT111, NRI, the N-terminal domain of NRI (NRI-N), and PII were purified as described previously (*18*, *26*, *27*). For gel filtration chromatography size standards, cytochrome *c* (12.5 kDa), chymotrypsinogen A (25 kDa), egg albumin (45 kDa), and bovine serum albumin (68 kDa) were used (Boehringer-Mannheim).

Construction of glnL Deletion Alleles and Gene Fusions. NT Series and CT190. The desired portion of *glnL* was amplified using the primers shown in Table 1. PCR conditions were as described previously (*28*). The upstream primers are designed to add an *Nde*I site overlapping the ATG start codon, and the downstream primers are designed to add an *Eco*RI or *Bam*HI site downstream of the termination codon. The PCR products were digested with *Nde*I and either *Eco*RI or *Bam*HI, as appropriate, and ligated into similarly cleaved pJLA503 (*29*). The entire sequence of the cloned fragment was determined by sequencing the resulting recombinant plasmids, using a Sequenase version 2.0 DNA sequencing kit (U.S. Biochemicals Corp.) according to the manufacturer's directions.

MBP Fusion Proteins (MBP−CT126, MBP−CT151, MBP−H_1, MBP−HX_2, and MBP−HX_3). The procedure was as outlined above, except that the PCR primers introduced an *Eco*RI site at the upstream end of the *glnL* sequence and a *Hin*dIII or *Bam*HI site downstream from the *glnL* sequence. PCR products were digested with *Eco*RI and either *Hin*dIII or *Bam*HI, and cloned into pMAL-c2 (New England Biolabs).

Purification of Truncated Forms of NRII. NT Series and CT190. The general strategy used to purify the polypeptides was as follows. Mid-exponential cells in LB medium with appropriate antibiotics (4 L) were induced to hyperexpress the desired protein by incubation at 44 °C for 4 h, as described previously (*26*). Overexpression in each case was sufficient to permit the direct visualization of the desired polypeptide by SDS−polyacrylamide gel electrophoresis; during purification, gel electrophoresis of aliquots was used to identify fractions containing the desired polypeptides. Cells were collected by centrifugation and stored as a frozen cell paste at −80 °C for 1−3 weeks. Frozen cells were thawed and resuspended in buffer A and disrupted by sonication in a Branson sonifier at 0−4 °C, and the extracts were clarified by centrifugation. Solid ammonium sulfate was added to the extracts at a sufficient concentration to just precipitate the desired protein. The concentration of ammonium sulfate required for each protein was determined by small-scale tests using aliquots of the extract. Ammonium sulfate precipitates were collected by centrifugation, dissolved and diluted with buffer B, and subjected to chromatography on DE52 (Whatman, preswollen microgranular grade) equilibrated in buffer B. After extensive washing of the columns, the desired proteins were eluted with a KCl gradient from 0 to 0.6 M in buffer B. Fractions containing the desired protein were pooled and concentrated by ammonium sulfate precipitation at a final concentration of 70% saturation (at 4 °C). The ammonium sulfate precipitates were collected by centrifugation, resuspended in a small volume (2−4 mL) of 50 mM Tris-HCl (pH 7.5), and subjected to gel filtration chromatography on Sephadex-G75 (Pharmacia) equilibrated in buffer A. For NT110, NT125, NT145, and NT155, these steps were sufficient to result in preparations that were ∼80−90% pure, as judged by gel electrophoresis. For these, the peak fractions were pooled, dialyzed against storage buffer (buffer S), and stored in aliquots at −80 °C. For NT135, NT169, and NT189, peak fractions from the gel filtration

column were pooled and subjected to phenyl-Sepharose chromatography. Depending on the protein, the samples were either loaded directly onto phenyl-Sepharose or brought to 0.5 M ammonium sulfate prior to loading the column. Columns were washed extensively and eluted with either a decreasing ammonium sulfate gradient or an increasing ethylene glycol gradient, depending on the protein. Peak fractions were pooled and dialyzed against storage buffer as described above.

MBP Fusion Proteins. Hyperexpression of the desired fusion proteins was achieved by induction with IPTG as described previously (*18*). Overexpression was sufficient in each case to permit detection by SDS gel electrophoresis, which was used to follow the course of purification. Frozen cells were resuspended in buffer A and disrupted by sonication, and the extracts were clarified by centrifugation. The fusion proteins were precipitated from the extracts with ammonium sulfate, resuspended in buffer E, and subjected to amylose affinity chromatography (New England Biolabs) according to the manufacturer's directions. Fusion proteins were eluted from the amylose resin with 10 mM maltose in buffer E. Peak fractions were pooled and subjected to gel filtration chromatography on BioGel A1.5 M (Bio-Rad) or on Sephadex G-75 (Pharmacia), depending on the mass of the desired protein. In all cases, the desired proteins were observed to elute as two peaks from gel filtration columns. The first peak contained aggregated material that eluted in the voided volume; the second peak corresponded to monomeric (MBP−CT151, MBP−H_1) or dimeric (the other samples) material. When the voided peak 1 material was subjected to a second round of gel filtration chromatography, it again eluted as two peaks corresponding to voided material and either monomeric or dimeric material, depending on the protein. Peak fractions were pooled and dialyzed against buffer S.

Buffers were as follows: (A) 50 mM Tris-HCl (pH 7.5), 200 mM KCl, 1 mM DTT, and 10% glycerol (v/v); (B) 50 mM Tris-HCl (pH 7.5), 1 mM DTT, and 10% glycerol; (E) 50 mM Tris-HCl (pH 7.5), 200 mM KCl, and 1 mM EDTA; and (S) 50 mM Tris-HCl (pH 7.5), 200 mM KCl, 1 mM DTT, and 50% glycerol (v/v).

Gel Electrophoresis. SDS−polyacrylamide gel electrophoresis, nondenaturing (simple) polyacrylamide gel electrophoresis, and urea denaturing polyacrylamide gel electrophoresis were performed as described previously (*23*). For pore-limit nondenaturing gel elctrophoresis, we used gradient gels [either 5% T (6% C) to 35% T (6% C) or 5% T (6% C) to 35% T (8% C), where T signifies total acrylamide (w/v) and C signifies the percentage of bis relative to total] at pH 8.9 without stacking gels. Voltage X time ranged from 2900 to 10 000 volt hours, at 4 °C. In pore-limit gel electrophoresis, polypeptides migrate to a position in the gradient gels where their further migration is sterically prevented by the limiting pore size. After this position has been reached, further electrophoresis leads to focusing of the bands at this position. The molecular mass of the polypeptides then can be deduced by comparisons with standards run on the same gradient gels.

Cleavage of MBP Fusion Proteins with Protease Factor Xa and Trypsin. MBP fusion proteins were cleaved with factor Xa (New England Biolabs) according to the vendor's directions, to liberate the NRII segments from MBP. After protease digestion, MBP and uncleaved fusion proteins were mostly removed by passing the reaction mixtures over amylose affinity columns. The flow-through material, corresponding to the NRII segments from the fusion proteins, was dialyzed against buffer S and stored at −80 °C in aliquots. This treatment typically did not completely remove the liberated MBP segement from the fusion proteins, as shown for the HX_3 polypeptide in Figure 3. Trypsin digestion conditions were 50 mM Tris-HCl (pH 7.5), 10 mM $MgCl_2$, 100 mM KCl, and various mass ratios of trypsin to target protein spanning a 10-fold range. Digestion was carried out at 23 °C for 10 min and stopped by addition of SDS gel loading buffer. For electrophoretic analysis, samples were separated on an SDS−14% polyacrylamide gel and stained with Coomassie brilliant blue R250.

Gel Filtration Chromatography for Estimation of Molecular Masses. A Sephadex G-75 column (95 cm × 1.1 cm, ∼48 mL bed volume) was used. The elution buffer consisted of 50 mM Tris-HCl (pH 7.5), 200 mM KCl, and 1 mM EDTA. Separation was carried out at 4 °C, and aliquots of fractions were examined on SDS gels to identify the elution volumes for each species. Blue dextran 2000 was used to determine the void volume (V_o) visually.

Subunit Exchange. Reaction mixtures contained 50 mM Tris-HCl (pH 7.5), 10 mM $MgCl_2$, 100 mM KCl, and the indicated proteins and were incubated at 4 °C for 69 h or at the indicated temperature for the indicated time interval. The samples were then subjected to nondenaturing gel electrophoresis on a 12 or 16% polyacrylamide gel, as indicated, and the protein bands were visualized by Coomassie brilliant blue R250 staining or by silver staining using a kit (Bio-Rad). For quantitation of staining intensities, Commassie brilliant blue-stained gels were scanned using a Fluor-S MultiImager (Bio-Rad), and the intensity of the bands was quantified with the Multi-Analyst program.

Autophosphorylation and Phospho Transfer Assays. Generally, the reaction conditions contained 50 mM Tris-HCl (pH 7.5), 10 mM $MgCl_2$, 100 mM KCl, 30 μM 2-ketoglutarate (or as indicated), 0.5 mM [γ-^{32}P]ATP (or as indicated), enzymes and substrates as indicated, PII as indicated, and NRI where indicated. Incubation was carried out at 25 °C or as indicated. For quantitative assessment by liquid scintillation counting, samples were removed from reaction mixtures at various times and spotted onto nitrocellulose filters, and the filters were washed extensively with either 5% TCA (for detecting NRI phosphorylation) or 0.1 M Na_2CO_3 (pH ∼11, for detecting NRII phosphorylation). Filters were then dried briefly and counted with liquid scintillation fluid. Errors using these assay methods were generally ≤10%. For analysis of reaction samples by SDS gel electrophoresis (Figure 8), reaction mixtures contained 0.1 mM [γ-^{32}P]ATP, and the reactions were stopped by addition of SDS loading buffer and heating at 85 °C for 5 min. SDS−14% polyacrylamide gels were used, and radioactive protein bands were detected by autoradiography of the wet gels at 4 °C. The protein bands were then stained with Coomassie brilliant blue R250, and the identities of the labeled bands in the autoradiograph were confirmed by comparison with the stained gels (not shown in Figure 8). For analysis of reactions by urea gel electrophoresis, reactions were stopped with urea as described previously (*23*).

Phosphatase Assays. Three different phosphatase assays were used. The first was essentially as described previously (*18*), except that 30 μM 2-ketoglutarate was included. In this assay, MBP−CT111, which has no phosphatase activity in the presence of PII (*18*), was used to phosphorylate NRI, present in excess. After incubation for 20 min at 25 °C, protein storage buffer, NRII, PII, or polypeptides derived from NRII were added as indicated. The extent of NRI phosphorylation was monitored at the indicated times by the TCA filter method described above. The second phosphatase assay was identical to the first, except that all protein components were present at the start of the reactions, which were initiated by addition of ATP. Errors using these assay methods were generally ≤10%. The third phosphatase assay measured the extent of dephosphorylation of NRI∼^{32}P in the absence of antagonistic phosphorylation. For this assay, NRI∼^{32}P was formed using MBP−CT111 as the kinase, and the reaction mixtures were subjected to gel filtration on Sephadex G-25 (Pharmacia) to remove small molecules. The voided fraction was then used as the NRI∼^{32}P substrate for dephosphorylation by added components as indicated. Reaction conditions were 50 mM Tris-HCl (pH 7.5), 10 mM $MgCl_2$, and 100 mM KCl at 25 °C. Errors using these assay methods were generally ≤15−20%.

Measurement of Glutamine Synthetase Expression in Intact Cells. The γ-glutamyl transferase activity of glutamine synthetase was measured as described previously (*25*). W-Salt-based defined medium was as described previously (*25*). Cultures from single-colony isolates were adapted in the indicated medium, subcultured to an OD_{600} of 0.02 and grown to an OD_{600} of 1. Strains YMC10 (wild-type) and RB9060 (Δ*glnB*) have been described (*30*). Strain BL (Δ*glnB*, *glnL2001*) was constructed in two steps. First, the *glnA::Tn5* mutation was introduced into strain RB9060 by phage P1vir-mediated generalized transduction (*31*), creating strain BA, which is a glutamine auxotroph. Strain BA was transduced to glutamine prototrophy with phage grown on strain RB9132 (*glnL2001*), which contains a null internal deletion in *glnL* (*30*). Prototrophic transductants were checked by PCR to ensure that they had inherited the *glnL2001* mutation. Cells were rendered competent and transformed with plasmid DNA by standard methods. Plasmid p*glnL*$^+$ is pgln62 described previously (*32*); this plasmid consists of the vector pBR322 with an insert bearing *glnL*$^+$ and the *glnL* promoter. Previous studies showed that *glnL*$^+$ from this plasmid complements a chromosomal *glnL2001* mutation for normal regulation of glutamine synthetase (*13*). Plasmid p*glnL*-H139N is isogenic to p*glnL*$^+$, except that it contains a point mutation altering histidine 139 to asparagine (*13*).

RESULTS

PII Is an Activator of the Phosphatase Activity of NRII. PII is an inhibitor of the NRII autophosphorylation reaction as well as an activator of the NRII phosphatase activity (*24*). One possible explanation for these observations was that the unphosphorylated form of the central domain of NRII was, by default, the phosphatase and that the role of PII in activating this activity was due to its ability to inhibit the autophosphorylation of NRII. Alternatively, PII might serve as an activator of the phosphatase activity, or might participate directly in this activity. To distinguish between these hypotheses, we assessed the ability of NRII to bring about the dephosphorylation of NRI∼^{32}P under conditions where ATP cleavage was prevented (Materials and Methods). NRII was a weak NRI∼P phosphatase in the absence of nucleotides, and this activity was increased by addition of the nonhydrolyzable ATP analogue, AMP-PNP (Figure 1). Thus, PII was not essential for the phosphatase activity. Addition of PII to the combination of NRI∼P, NRII, and AMP-PNP resulted in very rapid dephosphorylation of NRI∼P (Figure 1). This indicates that even under conditions where NRII was not autophosphorylated, PII was a potent activator of the phosphatase activity. In additional experiments, we observed that a slightly faster rate of dephosphorylation was obtained with NRII, PII, and ATP (data not shown).

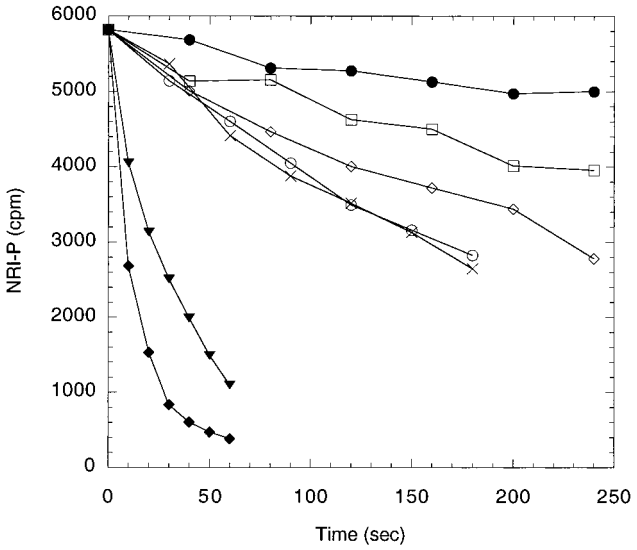

FIGURE 1: Effect of AMP-PNP and PII on the phosphatase activity of NRII and NRII-H139N. Reaction mixtures contained 0.11 μM NRI∼^{32}P (subunit concentration, ∼53000 cpm/μM), 10 mM $MgCl_2$, 30 μM 2-ketoglutarate, 0.3 mg/mL BSA, and the following additions: (●) none, (□) 0.3 μM NRII-H139N, (◇) 3 μM NRII, (○) 0.3 μM NRII-H139N and 1 mM AMP-PNP, (×) 3 μM NRII and 1 mM AMP-PNP, (▼) 0.3 μM NRII, 0.3 μM PII, and 1 mM AMP-PNP, and (◆) 0.3 μM NRII-H139N, 0.3 μM PII, and 1 mM AMP-PNP. Incubation was carried out at 25 °C. Preliminary experiments showed that in similar experiments, the presence of 1 mM ATP or 1 mM ATP and 0.3 μM PII did not alter the basal rate of NRI∼^{32}P dephosphorylation. The preparation of NRI∼^{32}P is described in Materials and Methods.

The mutant protein NRII-H139N is unable to be autophosphorylated, due to mutation of the H139 site of phosphorylation. Previous studies with this protein showed that it has elevated basal phosphatase activity in the absence of PII (*13*, *26*). In our experiments, the NRII-H139N protein appeared to have a ∼10-fold elevation of the basal phosphatase activity (Figure 1). This also suggests that PII was not directly involved in the activity. The NRI∼P phosphatase activity of NRII-H139N was dramatically stimulated when PII and AMP-PNP were present (Figure 1). Since NRII-H139N is altered at the site of NRII phosphorylation, the dephosphorylation of NRI∼P in this experiment cannot be due to the reversal of the kinase reaction. This conclusion was supported by thin-layer chromatography analysis of the reaction mixtures, which indicated that even when wild-type NRII was present, essentially all of the liberated phosphoryl groups appeared as P_i (data not shown). Since previous

Table 2: Glutamine Synthetase Expression in Adapted Cultures of *E. coli*

strain	glutamine synthetase transferase activity (nM min^{-1} mg^{-1})	
	glucose/glutamine medium[a]	glucose/ammonia/ glutamine medium[a]
YMC10 (wild-type)	1625	158
YMC10/p*glnL*$^+$	2281	158
YMC10/p*glnL*-H139N	83	75
RB9060 (Δ*glnB*)	2226	1201
RB9060/p*glnL*$^+$	2506	1245
RB9060/p*glnL*-H139N	1964	1086
BL (Δ*glnBglnL2001)*	2669	722
BL/p*glnL*$^+$	3342	1198
BL/p*glnL*-H139N	31	55

[a] The nitrogen-limiting glucose/glutamine medium contained 0.4% (w/v) glucose and 0.2% (w/v) glutamine. The nitrogen-excess glucose/ammonia/glutamine medium contained in addition 0.2% (w/v) ammonium sulfate.

results (*7*, *8*, *24*, *26*) and control experiments (data not shown) have shown that PII is not itself a phosphatase, our results suggest that PII is an activator of the phosphatase activity. We hypothesize that when PII binds, a conformation of NRII with potent phosphatase activity is stabilized.

The PII-dependent and PII-independent phosphatase activities of the NRII-H139N protein were also assessed in intact cells, by examining the ability of NRII-H139N to act as a negative regulator of *glnA* expression when it was expressed from a multicopy plasmid (Materials and Methods). Previous experiments have shown that expression of *glnA*, encoding glutamine synthetase (GS), is very sensitive to activation by NRI∼P. In wild-type cells, the phosphorylation state of NRI is primarily controlled by NRII, which is in turn regulated by PII. In cells lacking NRII (Δ*glnL*), acetyl phosphate brings about the phosphorylation of NRI, resulting in activation of *glnA* expression (*33*). Previous studies have shown that the level of acetyl phosphate is higher in ammonia-starved cells than in ammonia-replete cells, and that in ammonia-replete cells, NRII and PII are responsible for counteracting the phosphorylation of NRI by acetyl phosphate (*33*).

In wild-type cells, which contain NRII and PII, GS was regulated by ammonia, and addition of p*glnL*$^+$ resulted in a modest increase in the level of GS under nitrogen-limiting conditions (Table 2). In contrast, addition of p*glnL*-H139N to wild-type cells resulted in the inability to activate GS in response to nitrogen limitation (Table 2). Thus, under these conditions, the NRII-H139N protein was able to effectively antagonize NRII and acetyl phosphate.

In cells lacking PII due to the Δ*glnB* mutation, GS was elevated in both the presence and absence of ammonia, as expected (*30*), and the addition of p*glnL*$^+$ did not significantly alter the levels of GS (Table 2). Addition of p*glnL*-H139N to cells lacking PII resulted in only a modest decrease in the expression of GS (Table 2). Thus, in the absence of PII, the NRII-H139N protein could not effectively antagonize the phosphorylation of NRI by NRII and acetyl phosphate.

In cells lacking both PII and NRII, acetyl phosphate alone is responsible for the activation of GS expression, which is about 4-fold regulated by ammonia under the growth conditions that were used (cultures grown in these media to an OD_{600} of 1.0). Addition of p*glnL*$^+$ to such cells resulted in an increased level of expression of GS in the presence or absence of ammonia, while addition of p*glnL*-H139N to such cells resulted in the inability to activate *glnA* expression (Table 2). Thus, in the absence of PII and NRII, the H139N protein was able to effectively antagonize the activation of *glnA* by acetyl phosphate. Together, the results from Table 2 suggest that the NRII-H139N protein had both PII-independent phosphatase activity and PII-dependent phosphatase activity in intact cells, and that only the PII-dependent activity could effectively antagonize the kinase activity of the NRII encoded by the single-copy chromosomal gene.

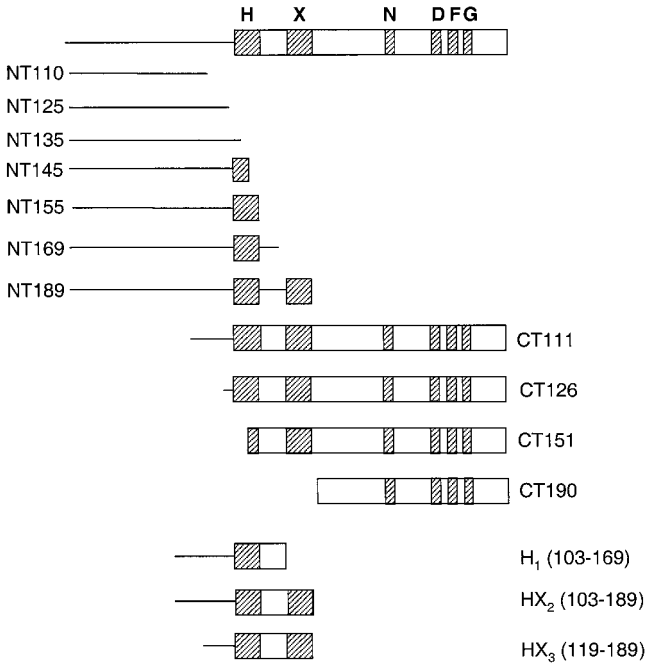

FIGURE 2: Truncated versions of NRII used in this study. A schematic depiction of NRII is shown at the top, followed by truncated versions of NRII. The N-terminal domain of NRII and the linker connecting the N-terminal domain to the transmitter module are depicted with a thin line. The conserved transmitter module of NRII is depicted as a thick line, and the positions of the conserved H-, X-, N-, D-, F-, and G-motifs are depicted as cross-hatched boxes.

Functional Dissection of the Activities of NRII and Their Regulation by PII. NRII exhibits four known activities. (i) It forms dimers in solution. (ii) It catalyzes its own phosphorylation on H139 (autophosphorylation) in a reaction where the rate and stoichiometry are regulated by PII. (iii) When phosphorylated, it serves as a source of phosphoryl groups for NRI phosphorylation (phospho transfer). (iv) When complexed with PII, it brings about the dephosphorylation of NRI∼P (phosphatase). To dissect the roles of various parts of NRII in these activities, we formed the series of truncated proteins depicted in Figure 2 and characterized their activities and the regulation of these activities by PII. We refer to polypeptides containing the N-terminus of NRII by the designation "NT" followed by the last amino acid in the polypeptide. We refer to polypeptides containing the C-terminus of NRII by the designation "CT" followed by the first amino acid found in the polypeptide. Internal polypeptides containing the H-box were also formed, and are designated "H" or "HX", depending on whether an intact X-box is also present (Figure 2). Each of the polypeptides depicted in Figure 2 was hyperexpressed and purified. The

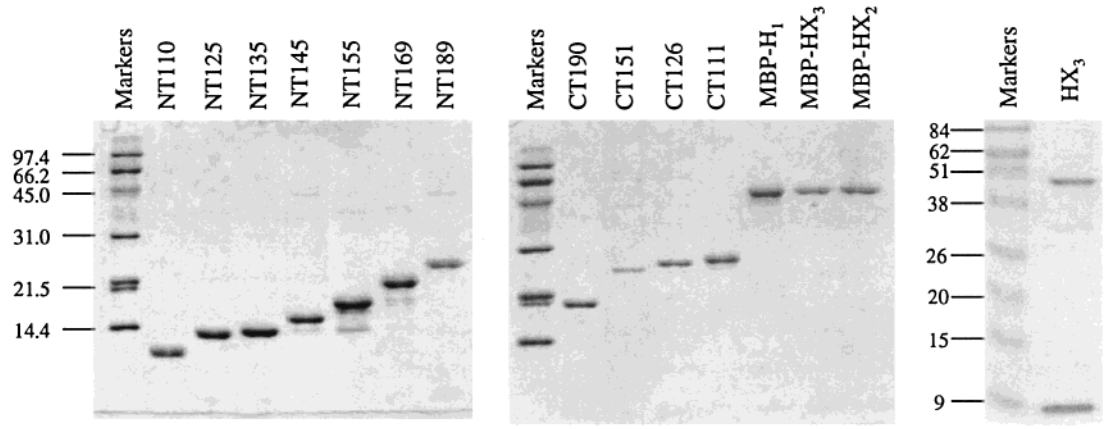

FIGURE 3: SDS−polyacrylamide gel electrophoresis of purified NRII truncations. Aliquots of each polypeptide were separated on a SDS−14% polyacrylamide gel, which was stained with Coomassie brilliant blue R250.

H and HX polypeptides were recalcitrant to overexpression and purification, as were CT111, CT126, and CT151; thus, these polypeptides were expressed as fusions to the C-terminus of the maltose-binding protein (MBP). To obtain the HX_3 (residues 119−189) polypeptide free from MBP−HX_3, the fusion protein was cleaved with protease factor Xa, followed by purification of the polypeptide to remove the bulk of the liberated MBP and uncleaved fusion protein. The CT111, CT126, and CT151 polypeptides were also purified as MBP fusions, cleaved from the fusion with protease factor Xa, and purified further to remove MBP [MBP−CT111 was previously described (*18*)]. The NT polypeptides and CT190 were expressed and purified without fusion to another protein. In some experiments, the MBP−CT, MBP−H_1, and MBP−HX fusion proteins were used, as indicated. SDS−polyacrylamide gels showing the purified polypeptides are presented in Figure 3.

Dimerization of NRII. NRII behaved like a dimer on gel filtration chromotography (*34*), on pore-limit gel electrophoresis (see below), and on nondenaturing polyacrylamide gel electrophoresis (see below). Previous results have indicated that dimers of NRII and MBP−NRII, a fusion protein consisting of the maltose-binding protein (MBP) fused to the N-terminus of NRII, could exchange subunits if a mixture of these proteins was subjected to denaturation with 2.8 M urea followed by dialysis (*22*). In our earlier experiments, no exchange of subunits between NRII and MBP−NRII was observed in the absence of urea for reaction mixtures that had been incubated for 1 min (*22*). We observed that upon longer incubation, NRII and MBP−NRII exchanged subunits spontaneously, forming heterodimers that contained one of each type of subunit (Figure 4A). In the experiment whose results are depicted in Figure 4A, where the incubation was carried out at 37 °C and each of the homodimers was initially present at 2 μM, the subunit exchange reaction approached the steady state within 2 h, at which point the heterodimers (qualitatively) constituted the expected fraction of the total staining intensity after staining of gels with Coomassie brilliant blue. The rate of subunit exchange was strongly affected by the temperature (Figure 4B). Exchange was most rapid at 42 °C, but at this temperature, significant losses of proteins occurred as revealed by material that failed to enter the gel or had a very high molecular mass. At ≤37 °C, significant losses of material did not occur. The rate of heterodimer formation at

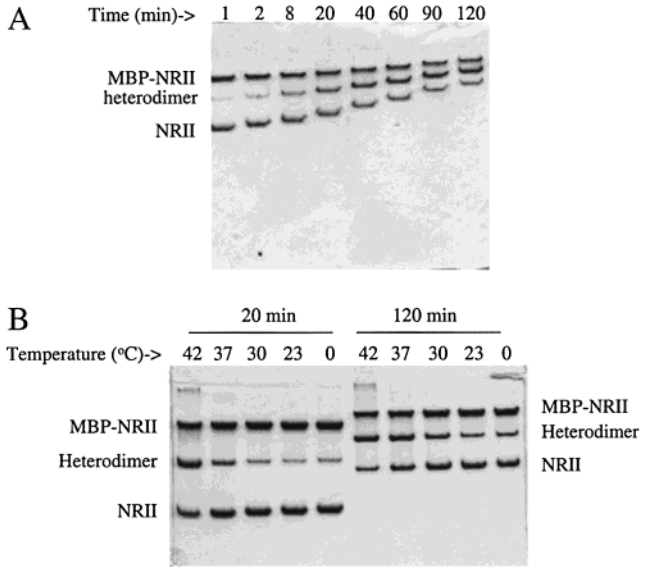

FIGURE 4: Subunit exchange between NRII and MBP−NRII dimers. (A) Time course of subunit exchange. MBP−NRII and NRII, 2 μM each, were incubated at 37 °C in 50 mM Tris-HCl (pH 7.5), 10 mM $MgCl_2$, and 100 mM KCl. At the indicated times, aliquots were removed and loaded onto a running 12% acrylamide nondenaturing gel. After good separation of the samples was achieved, the gel was stained with Coomassie brilliant blue R250. (B) Effect of temperature on subunit exchange. Conditions were as described for panel A, except that the indicated temperatures and times were used.

25 °C was similar to that seen at 0 °C (Figure 4B).

The subunit exchange reaction involving NRII and MBP−NRII was regulated by ATP and PII. In the presence of ATP or AMP-PNP, the rate of subunit exchange was inhibited slightly (Figure 5, 18% inhibition by ATP and 26% inhibition by AMP-PNP). Since the nonhydrolyzable AMP-PNP level was inhibitory, the binding of nucleotides by NRII appeared to result in a slightly slower rate of subunit exchange. The combination of PII, 2-ketoglutarate, and either ATP or AMP-PNP resulted in a dramatic inhibition of the rate of subunit exchange (Figure 5, 57% when AMP-PNP was used and 60% when ATP was used). This is consistent with the hypothesis that PII stabilizes the "phosphatase conformation" of NRII, and implies that when so stabilized, NRII is not able to undergo subunit exchange.

Dimerization Determinants in NRII and Domain Organization of NRII. To define the portion(s) of NRII responsible

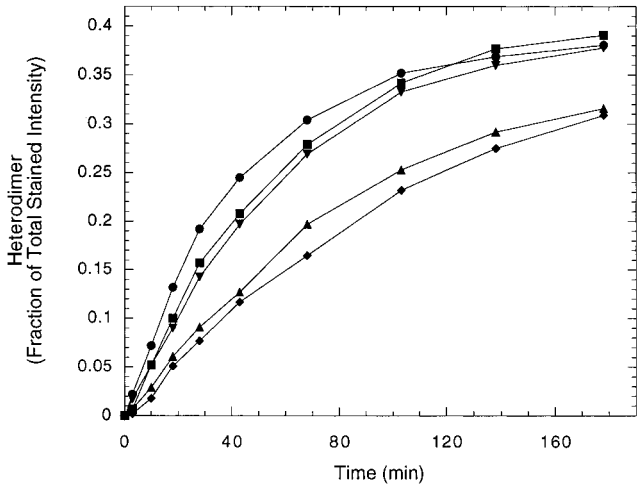

FIGURE 5: Regulation of NRII subunit exchange by PII and nucleotides. Reaction conditions were as described in the legend of Figure 4, except that MBP−NRII and NRII were at 5 μM each, and ATP or AMP-PNP was at 3 mM, PII was at 20 μM, and 2-ketoglutarate was at 50 μM, where indicated. Samples were resolved on 12% acrylamide nondenaturing gels, stained with Coomassie brilliant blue R250, and scanned with a Flour-S MultiImager (Bio-Rad), and the intensity of the bands was quantified using the Multi-Analyst program. The fraction of total staining intensity of the heterodimer band is plotted as a function of time. Symbols with rate in parentheses (fraction of total staining intensity per minute): (●) control with no PII or nucleotide (0.00692), (■) ATP (0.00578), (▼) AMP-PNP (0.00506), (▲) PII, AMP-PNP, and 2-ketoglutarate (0.00305), and (◆) PII, ATP, and 2-ketoglutarate (0.00284).

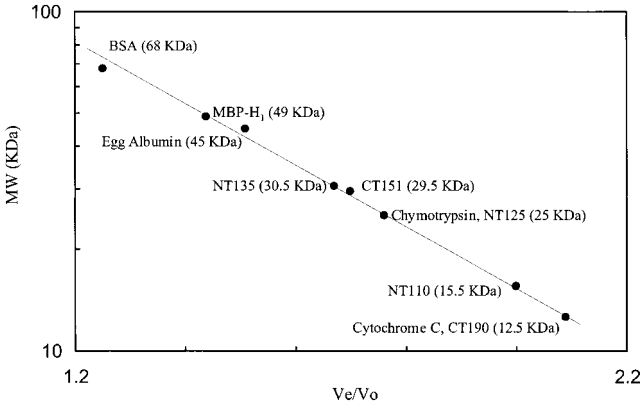

FIGURE 6: Sephadex G-75 gel filtration chromatography of NRII truncations. The conditions were as described in Materials and Methods. The data that are shown were from three separate experiments with the same column and conditions. The protein standards (BSA, egg albumin, chymotrypsinogen A, and cytochrome *c*) were eluted at identical V_e/V_o values in the three experiments, and NT125 was assayed twice with identical results.

for dimerization and subunit exchange, we examined the polypeptides shown in Figure 2. Gel filtration chromatography was performed on Sephadex G-75 for selected polypeptides (Figure 6). The results of these experiments unambiguously indicated that NT110, CT190, and MBP−H_1 were monomeric and NT125 and NT135 were dimeric. CT151 was unusual, in that it eluted from gel filtration columns at a volume corresponding to a mass intermediate between those of its monomeric and dimeric forms. The mobilities of these species were examined on nondenaturing gels and compared to those of the other species (data not shown). Mobility in nondenaturing gel electrophoresis is affected by size and charge, so no simple correspondence between mobility and molecular mass exists. Nevertheless, the difference in migration between monomers and dimers was generally sufficient to permit an unambiguous determination. All of the polypeptides migrated as well-defined bands upon nondenaturing gel electrophoresis with the single exception of CT 151, which reproducibly ran as a broad smear. While MBP−NRII appeared to be mostly dimeric, MBP−CT111, MBP−CT126, and MBP−CT151 each demonstrated the presence of higher-molecular mass aggregates. By this analysis, MBP−CT111 and MBP−CT126 appeared to be mostly dimers, while MBP−CT151 appeared to be mostly monomeric. All of the NT species appeared to be dimeric except NT110, which appeared to be monomeric. CT111 and CT126 were dimers, while CT190 was monomeric. The status of CT151 could not be determined by this method, as noted above. Significantly, MBP−HX_2 and MBP−HX_3 appeared to be dimeric, indicating residues 119−189 were sufficient to bring about the dimerization of MBP. Since MBP−H_1 appeared to be monomeric (Figure 6, data not shown), residues 169−189 (the X-box region) were required for the dimerization of MBP by fusion with H-box regions of NRII.

As another test of the oligomeric state of the polypeptides, pore-limit electrophoresis was performed. In pore-limit gels, polypeptides migrate to an equilibrium position in the gradient gel where their further migration is prevented (Materials and Methods). The results of pore-limit gel analysis were consistent with the results presented above. NT110, CT190, and CT151 were monomeric, and the remainder of the NT and CT series were dimeric. MBP−H_1 was monomeric, and MBP−HX_2 and MBP−HX_3 were dimeric (data not shown).

The domain organization of NRII may be surmised on the basis of the available information for related proteins (introductory section), by sequence inspection (*2*), and the properties of the polypeptides described above. NRII appears to consist of three domains, with two linkers connecting them. The N-terminal domain consists of residues ∼1−110. A linker is formed by residues ∼111−126. A central dimeric domain containing the four-helix bundle comprises residues ∼126−189. A linker and the C-terminal domain are comprised of residues 190−349. The H−X region of NRII appeared to form a distinct domain. In the course of our studies on cleavage of MBP−HX_3 with protease factor Xa, we examined the cleavage of this fusion protein with trypsin. SDS−polyacrylamide gel electrophoresis of cleavage products indicated that under the appropriate conditions, trypsin released the HX segment nearly as well as did factor Xa (data not shown). Since a potential trypsin site is within the H-box motif, and this trypsin site is cleaved in denatured NRII (*3*) and upon exposure to a very high trypsin concentration (data not shown), this trypsin site must be fairly inaccessible due to the structure of the dimeric H−X segment.

Regions of NRII Required for Subunit Exchange. We used the series of truncated proteins to determine which portions of NRII were required for the ability to undergo subunit exchange with wild-type (full-length) NRII or MBP−NRII. Of the constructs shown in Figure 2, only NT189 was able to undergo subunit exchange with NRII or MBP−NRII to detectable levels (Figure 7 and data not shown). This shows that the subunit exchange activity of intact NRII was not an

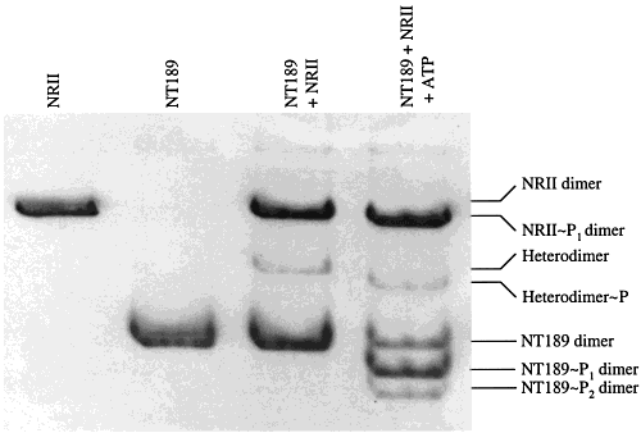

FIGURE 7: Subunit exchange between NRII and NT189 and formation of doubly phosphorylated NT189 dimers. The conditions were as described in Materials and Methods. A 16% polyacrylamide nondenaturing gel was used.

intrinsic property of the central, dimerization, domain of NRII, but required the presence of the N-terminal domains. Indeed, the isolated central domain (MBP−HX_3 and HX_3) and transmitter module (CT111 and CT126) of NRII formed stable dimers that did not undergo detectable subunit exchange. The formation of heterodimers of NRII and NT189 was at least 1 order of magnitude slower than the formation of heterodimers of NRII and MBP−NRII (data not shown). Also, the yield of heterodimers in experiments with NRII and NT189 was low at equilibrium (data not shown), suggesting that NRII dimers or NT189 dimers (or both) were more stable than NRII::NT189 heterodimers. Together, the results suggested that in full-length NRII, interactions between the N-terminal and kinase domains of NRII destabilize the dimeric central domain, favoring the subunit exchange reaction.

Previous results have indicated that upon addition of ATP, NRII dimers have slightly greater mobility on nondenaturing gels (ref *23* and Figure 7). Extensive gel analysis of this alteration has suggested that only a single phosphorylated NRII species was detected in similar experiments, even when doubly phosphorylated NRII was loaded onto the gel, and that this species corresponded to the hemiphosphorylated species (ref *23* and unpublished data). One explanation for these results is that the doubly phosphorylated NRII dimer, known to be unstable in solution (*23*), rapidly decays to the hemiphosphorylated species soon after it is loaded onto the gel. Yet, we observed that when ATP was present along with NRII and NT189, doubly phosphorylated NT189 dimers were clearly detected on nondenaturing gels as a band with faster migration than hemiphosphorylated NT189 dimers (Figure 7 and data not shown). This result suggests that removal of the kinase domain removes an impediment to the accumulation of the doubly phosphorylated dimer or, more likely, renders such dimers more stable during electrophoresis.

Autophosphorylation and Transphosphorylation Activities of NRII Truncations. We examined the ability of the polypeptides shown in Figure 2 to become autophosphorylated upon incubation with ATP, their ability to become phosphorylated when mixed with ATP and NRII (or an active truncated form of NRII), and the regulation of these phosphorylation reactions by PII. Previous results from studies of NRII (*20*), EnvZ (*10*), and CheA (*19*) have indicated that the phospho-accepting histidine may become phosphorylated when present on a short polypeptide in the presence of the intact kinase or a truncated form of the kinase bearing the kinase domain. Similarly, we previously observed that a truncation of NRII, NT202 (using the terminology employed here), could be phosphorylated by intact NRII (*22*).

Table 3: Oligomeric State, Autokinase, Kinase, Phospho-Accepting, and Phosphatase Activities of NRII Truncations

polypeptide	oligomer[a]	autokinase	kinase	phospho-accepting	phosphatase
NT110	m	−	−	−	−
NT125	d	−	−	−	−
NT135	d	−	−	−	−
NT145	d	−	−	−	−
NT155	d	−	−	−	−
NT169	d	−	−	+[b]	−
NT189	d	−	−	+[c]	+
CT111	d	+	+[d]	NT[e]	+
CT126	d	+	+[d]	NT[e]	+
CT151	m/d	−	+[d]	−	−
CT190	m	−	+[f]	−	−
MBP−H_1	m	−	−	−	−
MBP−HX_2	d	−	−	+[c]	+
MBP−HX_3	d	−	−	+[c]	+
HX_3	d	−	−	+[c]	+

[a] m, monomer; d, dimer. [b] Phosphorylated by WT, CT111, CT126, and CT151. [c] Phosphorylated by WT, CT111, CT126, CT151, and CT190. [d] Able to phosphorylate NT189, MBP−HX_2, MBP−HX_3, NT169, and HX_3. [e] Not tested. [f] Able to phosphorylate NT189, MBP−HX_2, MBP−HX_3, and HX_3.

The results of our analysis are summarized in Table 3, and representative autoradiographs are presented in Figure 8. The NT110, NT125, NT135, NT145, and NT155 polypeptides were not autophosphorylated upon incubation with ATP, and could not be phosphorylated by wild-type NRII. Among these, the latter two polypeptides contain active site histidine 139 but are nevertheless completely inactive. NT169 was not autophosphorylated, but could become phosphorylated when mixed with wild-type NRII. NT169 was poorly phosphorylated by CT111, CT126, and CT151, and was not phosphorylated by CT190 (Figure 8). Curiously, when a 5-fold higher concentration of CT151 was used, the extent of phosphorylation of NT169 was increased more than 5-fold (Figure 8). Thus, for CT151 at low concentrations (1 μM), the low kinase activity toward NT169 may reflect a dimerization defect in CT151. NT189 was not autophosphorylated; it could be phosphorylated by NRII and by each of the CT polypeptides at approximately equal rates (Figure 8). Thus, among the NT series of polypeptides, only NT169 and NT189 could be phosphorylated, and of these, the NT189 protein was the more promiscuous phospho acceptor (Figure 8 and Table 3).

Among the CT series of polypeptides, only CT111 and CT126 contain the active site histidine 139. These two polypeptides were autophosphorylated when incubated with ATP. All four proteins of the CT series (CT111, CT126, CT151, and CT190) could phosphorylate NT189 (Figure 8), MBP−HX_2 (not shown) and MBP−HX_3 (not shown), and the isolated HX_3 polypeptide (Figure 8). MBP−H_1 could not be phosphorylated by wild-type NRII, CT111, CT126, CT151, or CT190. Thus, the X-box region was required (that is, an intact H−X region was required) for phosphorylation of the H-box in the MBP−H context. Surprisingly, CT111

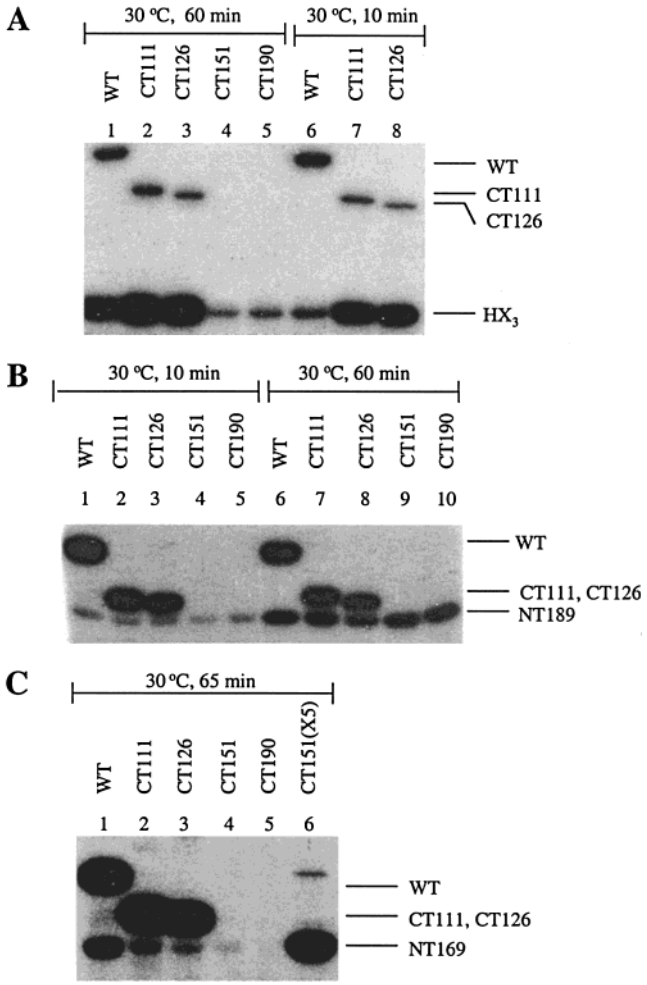

FIGURE 8: Autophosphorylation and phospho-accepting activities of NRII truncations. The conditions and procedures were as described in Materials and Methods and on the panels; only the autoradiographs are shown. In the experiments whose results are depicted in each panel, the concentration of [γ-^{32}P]ATP was 0.1 mM, and enzyme concentrations were 1 μM except as indicated. (A) Phosphorylation of HX_3 by various NRII polypeptides. HX_3 was present at 10 μM in each reaction mixture. (B) Phosphorylation of NT189 by various NRII polypeptides. NT189 was present at 8 μM in each reaction mixture. (C) Phosphorylation of NT169 by various NRII polypeptides. NT169 was present at 10 μM in each reaction mixture. The lane designated CT151 (X5) contained 5-fold more kinase (5 μM) than the other lanes.

and CT126 were considerably more active in phosphorylating MBP−HX_2 and MBP−HX_3 than was NRII (not shown), and CT111 and CT126 were similarly more active than NRII in phosphorylating the isolated HX_3 polypeptide (Figure 8). This indicates that the N-terminal domain of NRII reduces the transphosphorylation activity, perhaps by limiting access to the active site by the central domain of NRII provided in trans.

To determine if the phosphorylation events we observed were due to phosphorylation of the active site His-139, we examined whether phosphorylated species could transfer phosphoryl groups to NRI. In every case where a phosphorylated NRII species was formed, the phosphoryl groups could be transferred to NRI (data not shown). This suggests that all of these phosphoryl groups were indeed due to the phosphorylation of His-139, and is consistent with the hypothesis that NRI catalyzes the transfer of phosphoryl groups from NRII−H139∼P to itself. However, we noticed

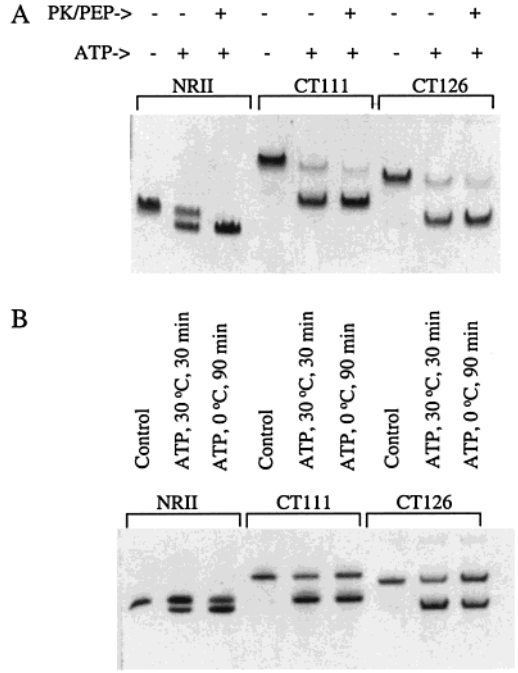

FIGURE 9: Stoichiometry of autophosphorylation. (A) Effect of PK and PEP on the stoichiometry of autophosphorylation of NRII, CT111, and CT126. Conditions were as described in Materials and Methods, and where indicated, ATP was at 0.5 mM, pyruvate kinase (PK) at 48 units/mL, and phosphoenolpyruvate (PEP) at 2 mM. Incubation was carried out at 25 °C for 40 min; then urea was added to a final concentration of 4 M, and the samples were resolved on a 10% polyacrylamide/6 M urea gel, which was carried out at 260 V for 2.5 h. The bands were visualized by Coomassie brilliant blue R250 staining. (B) Effect of temperature on the stoichiometry of autophosphorylation. Conditions were similar to those described for panel A, except that ATP, where included, was 0.1 mM for wild-type NRII and 0.5 mM for CT111 and CT126.

that dephosphorylation of NT169∼P by NRI was considerably slower than dephosphorylation of the other species (data not shown), suggesting that the phosphoryl groups in NT169∼P were less accessible to NRI than in the other cases.

The stoichiometry of autophosphorylation was compared for CT111, CT126, and NRII by urea gel electrophoresis. These denaturing gels, which contain urea in place of the typically used SDS, resolve phosphorylated and unphosphorylated NRII subunits and are therefore useful for qualitative assessments of the stoichiometry of autophosphorylation (*23*). In experiments where autophosphorylation occurred at 25 °C for 40 min with ATP at 0.5 mM, about half of the available sites in NRII were phosphorylated, but essentially complete phosphorylation of the available sites was obtained when an ADP-consuming system consisting of pyruvate kinase and PEP was present (Figure 9A), as shown previously (*23*). However, under these conditions, the extent of autophosphorylation of CT111 and CT126 was clearly greater than that of NRII, and little further phosphorylation of CT111 and CT126 subunits was obtained by inclusion of PK and PEP (Figure 9A). This suggests that under these conditions, most of the active CT111 and CT126 subunits were phosphorylated. However, at reduced ATP concentrations, a lower stoichiometry of CT111 and CT126 autophosphorylation was observed, and under these conditions, inclusion of PK and PEP increased the stoichiometry of CT111 and CT126 autophosphorylation to completion (Figure 10, upper panel). This indicates that the asymmetry of NRII autophosphorylation

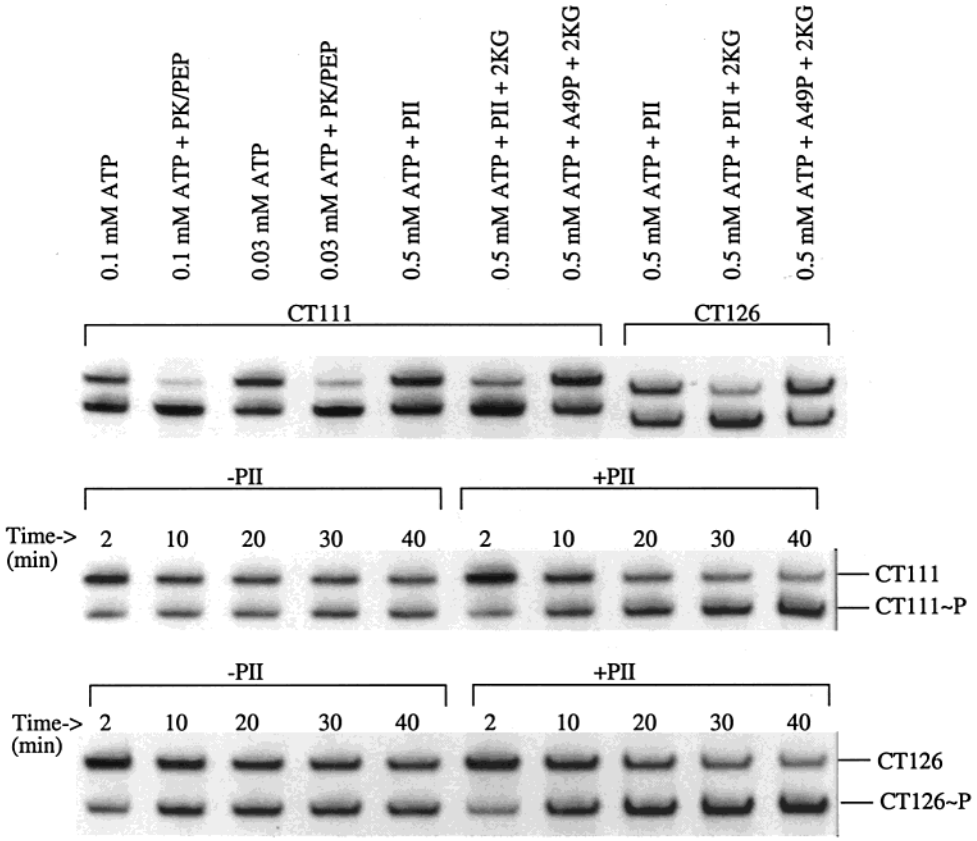

FIGURE 10: Effect of PII on the autophosphorylation of CT111 and CT126. (Top) Effect of PII and the combination of PK and PEP on the stoichiometry of autophosphorylation. Reaction conditions and urea−acrylamide gel electrophoresis were as in Figure 9 except as follows. For the four left lanes, incubation was carried out at 25 °C for 40 min, and for the six right lanes, incubation was carried out at 0 °C for 40 min. Where indicated, PII was at 16 μM, 2-ketoglutarate at 30 μM, PK at 48 units/mL, and PEP at 2 mM. A49P signifies PII-A49P, which contains the alteration of alanine at position 49 to proline. This mutant form of PII retains other PII activities, but does not interact with NRII (*28*). Time courses of CT111 autophosphorylation (middle panel) and CT126 autophosphorylation (bottom panel) were similar to Figure 9; ATP was at 0.5 mM and 2-ketoglutarate at 30 μM, and where indicated, PII was at 16 μM. For all three panels, only the portion of the urea−acrylamide gel showing the NRII, CT111, and CT126 subunits is shown.

is partially reduced by removal of the N-terminal domain. Decreasing temperatures resulted in an increase in NRII autophosphorylation stoichiometry and a decrease in CT111 and CT126 autophosphorylation stoichiometry (Figure 9B); that is, the temperature effect on autophosphorylation stoichiometry was reversed upon deletion of the N-terminal domain. By manipulation of temperature, time, and ATP concentration, various equilibrium extents of autophosphorylation could be obtained (Figure 9B and data not shown).

PII Increases the Stoichiometry of Autophosphorylation of CT111 and CT126. We examined the effect of the PII protein on the autophosphorylation of CT111 and CT126. Previous results have shown that PII inhibits the rate of autophosphorylation of NRII (*24*) but under certain conditions increases the stoichiometry of NRII autophosphorylation (*23*).

As already noted, at 0 °C the autophosphorylation of CT111 and CT126 was slow, and about half of the available sites were phosphorylated at equilibrium when the ATP concentration was 0.5 mM. Addition of PII resulted in a significant increase in autophosphorylation stoichiometry under these conditions, as indicated by urea gel analysis (Figure 10). This increase in the extent of autophosphorylation of CT111 and CT126 was not due to nonspecific effects of PII as indicated by two types of control experiments. First, addition of the PII-A49P protein in place of PII eliminated the stimulation; PII-A49P was previously shown to completely lack the ability to interact with NRII but retained the other activities of PII [2-ketoglutarate and ATP binding, uridylylation by UTase/UR, and activation of ATase (*28*)]. Second, stimulation of autophosphorylation required 2-ketoglutarate; previous studies have shown that 2-ketoglutarate at the concentration used is a potent allosteric activator of PII that enables it to bind to NRII (*27*, *35*). The time course of autophosphorylation of CT111 and CT126 (Figure 10) indicated that the presence of PII had little effect on the initial rate of autophosphorylation, but dramatically affected the stoichiometry of autophosphorylation. To confirm the urea gel results, experiments with labeled ATP were performed to directly measure the extent of autophosphorylation of CT111 and CT126; the results of these experiments also indicated that PII significantly increased the stoichiometry of autophosphorylation of CT111 and CT126, but did not increase the initial rates of autophosphorylation (data not shown). Since PII increased the extent of autophosphorylation of the CT111 and CT126 polypeptides, PII must interact with the transmitter module of NRII. Furthermore, PII slightly increased the rate and steady-state extent of NRI phosphorylation by CT111 and CT126 (data not shown). This latter effect was most dramatic for CT126, and we will show below that this difference between CT111 and CT126 was due in part to CT111 having weak NRI∼P phosphatase activity, while CT126 had less of this activity.

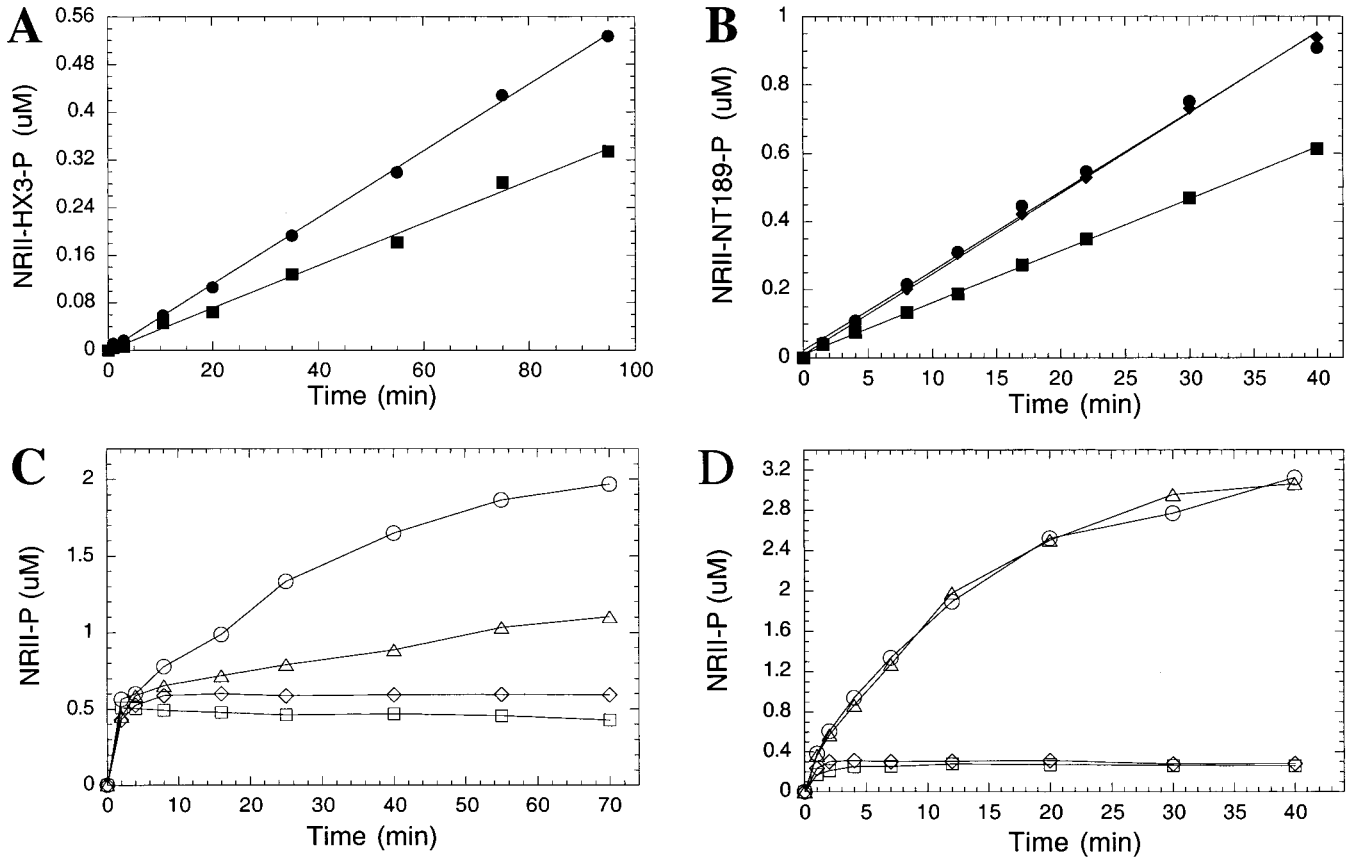

FIGURE 11: Effect of PII on the transphosphorylation activities of CT190, NRII, and CT111. Phosphorylation of histidine residues was monitored by the Na_2CO_3 filter method and liquid scintillation as described in Materials and Methods. (A) Effect of PII on transphosphorylation of HX_3 by CT190. Reaction mixtures contained 0.5 mM [γ-^{32}P]ATP, 6 μM HX_3, 3 μM CT190, 12 μM PII where indicated, 30 μM 2-ketoglutarate, and 0.5 mg/mL BSA. The rates in this experiment from linear regression analysis were 5.55 $\pm$ 0.05 nM/min in the absence of PII and 3.55 $\pm$ 0.09 nM/min in the presence of PII, indicating 36% inhibition by PII: (●) without PII and (■) with PII. (B) Effect of PII on transphosphorylation of NT189 by CT190. Reaction mixtures contained 0.5 mM [γ-^{32}P]ATP, 10 μM NT189, 4 μM CT190, 12 μM PII where indicated, 30 μM 2-ketoglutarate where indicated, and 0.5 mg/mL BSA: (■) with PII and 2-ketoglutarate, (◆) with PII and without 2-ketoglutarate, and (●) without PII and with 2-ketoglutarate. The rates from linear regression anaylsis were 23.28 nM/min in the absence of PII and 23.63 nM/min in the presence of PII and absence of 2-ketoglutarate. In the presence of PII and 2-ketoglutarate, the rate was 15.20 nM/min, indicating a 35% inhibition by PII. (C) Effect of PII on transphosphorylation of HX_3 by wild-type NRII. Reaction mixtures contained 0.5 mM [γ-^{32}P]ATP, 6 μM HX_3 where indicated, 0.6 μM NRII, 12 μM PII where indicated, 30 μM 2-ketoglutarate, and 0.5 mg/mL BSA: (□) NRII alone, (◇) NRII and PII, (○) NRII and HX_3, and (△) NRII, PII, and HX_3. The *Y*-axis indicates total molarity of phosphoryl groups incorporated into both HX_3 and NRII. The initial rates of transphosphorylation of HX_3 by NRII were 41.76 nM/min in the absence of PII and 8.33 nM/min in the presence of PII after correction by subtraction of the phosphoryl groups from autophosphorylation of NRII. Thus, PII caused an 80% inhibition of transphosphorylation. (D) Effect of PII on the transphosphorylation of HX_3 by CT111. Reaction mixtures contained 0.5 mM [γ-^{32}P]ATP, 6 μM HX_3 where indicated, 0.6 μM CT111, 12 μM PII where indicated, 30 μM 2-ketoglutarate, and 0.5 mg/mL BSA: (□) CT111 alone, (◇) CT111 and PII, (○) CT111 and HX_3, and (△) CT111, HX_3, and PII. The *Y*-axis indicates the total molarity of phosphoryl groups incorporated into both HX_3 and CT111.

PII Inhibits the Kinase Activity of the Isolated Kinase Domain of NRII. We examined the effect of PII on the phosphorylation of NT189 and the HX_3 polypeptide by the isolated kinase domain of NRII (CT190). PII was a weak inhibitor of these transphosphorylation reactions but, when present at a sufficient concentration, caused significant inhibition (36% inhibition under the conditions used in the experiments whose results are depicted in Figure 11A and three additional experiments employing similar conditions, 35% inhibition under the conditions used in the experiments whose results are depicted in Figure 11B and one additional experiment under the same conditions). Inhibition by PII was observed in the presence of a vast excess of BSA, and thus was not due to bulk effects (Figure 11). The inhibition by PII depended on 2-ketoglutarate (Figure 11B), as expected. Since PII can inhibit the transphosphorylation activity of the isolated kinase domain of NRII, the kinase domain is likely the site of PII interaction with NRII.

PII was a very potent inhibitor of the transphosphorylation of the HX_3 polypeptide by wild-type NRII (Figure 11C). At the same PII concentration that provided ~36% inhibition of the CT190 transphosphorylation activity, ~80% inhibition of NRII transphosphorylation activity was observed. However, when CT111 was used as the kinase for transphosphorylation of the HX_3 polypeptide, PII did not affect the rate of transphosphorylation (Figure 11D). Since CT111 and NRII autophosphorylation is also detected in these experiments, a limiting concentration of CT111 or NRII was used along with excess HX_3 polypeptide with or withour excess PII. If the inhibition seen with the isolated kinase domain also occurs with CT111, it must be balanced by an activation of transphosphorylation that is seen with the isolated transmitter module (CT111) but not with the isolated kinase domain (CT190) or with intact NRII. Similarly, PII inhibition of NRII transphosphorylation activity cannot be explained by simple inhibition of the kinase domain, and must involve

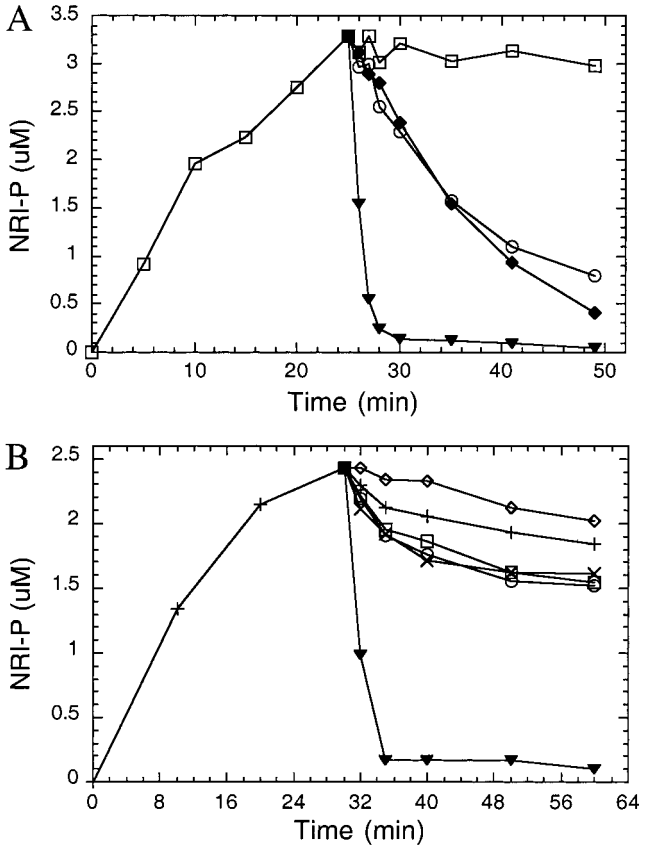

FIGURE 12: Phosphatase activities of NRII truncations. (A) Phosphatase activity of NRII and NT189. The initial reaction conditions included 50 mM Tris-HCl (pH 7.5), 10 mM $MgCl_2$, 100 mM KCl, 50 μM 2-ketoglutarate, 12 μM NRI, 0.3 μM MBP−CT111, and 0.5 mM [γ-^{32}P]ATP. After incubation at 25 °C for 25 min, additions were (□) protein storage buffer, (○) 8.1 μM NT189, (◆) 8.1 μM NT189 and 5.1 μM PII, and (▼) 0.3 μM NRII and 2.5 μM PII. Previous experiments have shown that addition of similar amounts of PII in the absence of NRII had no effect (*18*). (B) Phosphatase activities of H-region truncations. The conditions were similar to those described for panel A, except that 2-ketoglutarate was at 30 μM, BSA was at 0.3 mg/mL, and the additions were carried out at 30 min. Additions were (+) protein storage buffer, (◇) 4.7 μM MBP−H_1, (□) 4.7 μM MBP−HX_3, (○) 3.5 μM HX_3, (×) 4.7 μM MBP−HX_2, and (▼) 0.3 μM NRII and 0.3 μM PII.

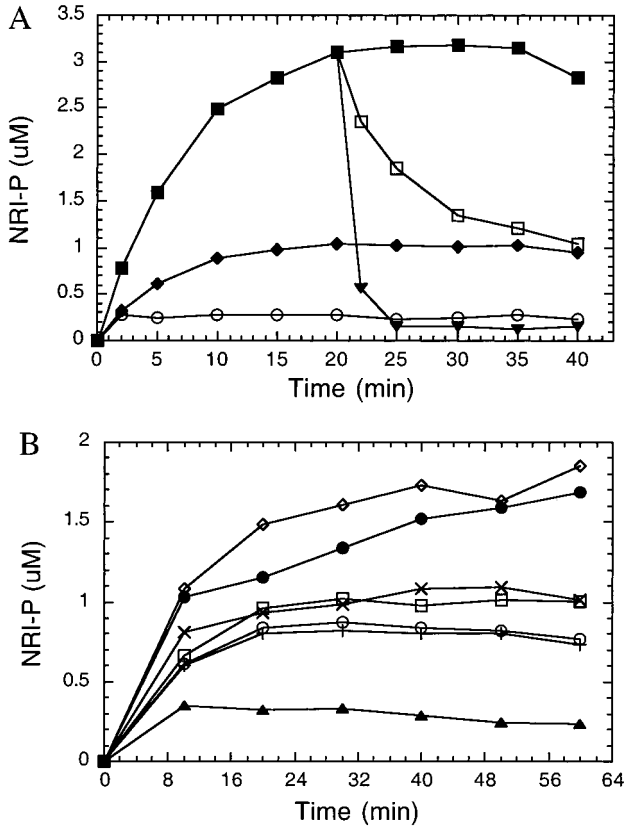

FIGURE 13: Effect of NRII truncations on the phosphorylation of NRI by MBP−CT111. (A) Experiment showing that the final steady-state level of NRI phosphorylation reflects the balance of the kinase and phosphatase activities. Conditions were as described in the legend of Figure 12, except NRI was at 10 μM, NRII was at 0.3 μM, and 2-ketoglutarate was at 50 μM: (■) no PII, (□) 0.03 μM PII added at 20 min, (◆) 0.03 μM PII added at time 0, (O) 0.3 μM PII added at time 0, and (▼) 0.3 μM PII added at 20 min. (B) Phosphatase activities of H-region truncations. The reaction conditions were as described in the legend of Figure 12B, except that all protein components were present from time 0: (◇) 10 μM MBP−H_1, (●) protein storage buffer, (× and □) 10 μM MBP−HX_2 but from different preparations, (+) 10 μM MBP−HX_3, (○) 10 μM HX_3, and (▲) 0.3 μM NRII and 0.3 μM PII.

regulation of the NRII conformation by PII. This conformational regulation apparently required the N-terminal domain of NRII.

Phosphatase Activity of NRII Truncations. The ability of the various truncated NRII polypeptides to bring about the dephosphorylation of NRI∼P was assessed. In one set of experiments, the MBP−CT111 protein was used to phosphorylate NRI, and when the level of NRI phosphorylation had achieved a steady state, either buffer or an NRI truncation was added, along with PII or PII storage buffer. Previous work has shown that MBP−CT111 lacks phosphatase activity, as does PII, and that addition of NRII and PII results in the rapid dephosphorylation of NRI∼P (*18*). This assay is convenient, since it does not require the purification of NRI∼P, but it does not directly measure the phosphatase activity but rather measures the balance between the kinase activity of MBP−CT111 (and any added species) and the phosphatase activity. Using this assay, we observed that, of the polypeptides depicted in Figure 2, only NT189, MBP−HX_2, MBP−HX_3, and the isolated HX_3 polypeptide exhibited significant phosphatase activity, and this activity was not activated by PII (Figure 12 and Table 3). Of these, NT189 clearly had the most potent phosphatase activity, and this activity was considerably lower than that observed with NRII and PII (Figure 12A).

Another way to measure the phosphatase activity of NRII is to include PII in the reaction mixtures from the start. To show that this assay measures the balance of the kinase and phosphatase activity of NRII, we examined the effect of adding PII either from the start or after wild-type NRII had been allowed to phosphorylate NRI for 20 min (Figure 13A). As shown, the final steady-state level of NRI phosphorylation was the same in the two assay mixtures, suggesting that this final steady-state level reflects the balance between the kinase and phosphatase activities in the reaction mixture. Thus, the final steady-state level of NRI phosphorylation could be used to assess the phosphatase activity of NRII in the presence of PII, and the phosphatase activity of various polypeptides derived from NRII. We included the polypeptides in Figure 2 (from time zero) in reaction mixtures containing MBP−CT111, excess NRI, and ATP, and assessed the final steady-state extent of NRI phosphorylation. Under these conditions, MBP−HX_2, MBP−HX_3, and the isolated HX_3 polypeptide

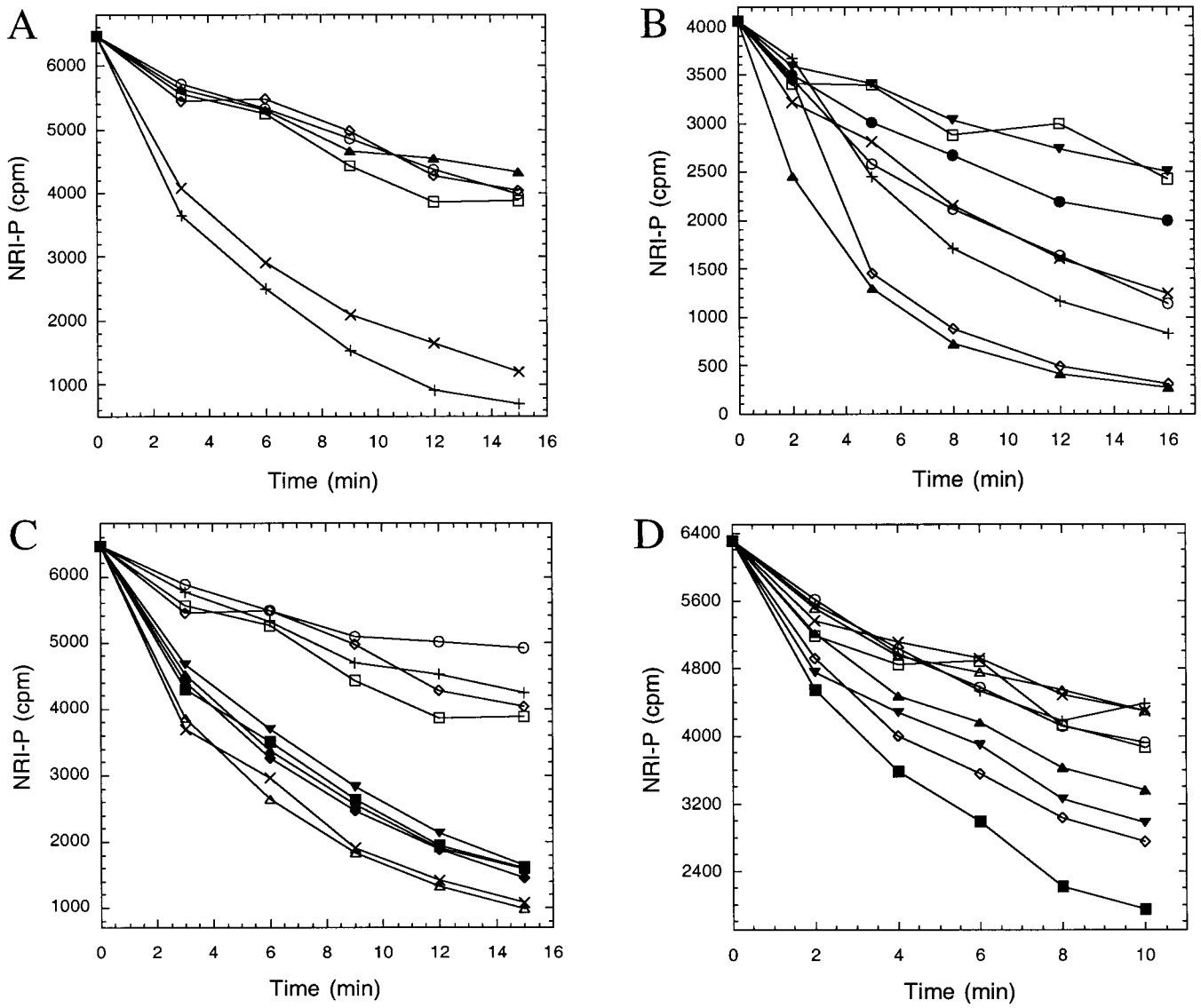

FIGURE 14: Effect of ATP and AMP-PNP on phosphatase activities. Reaction conditions were as described in the legend of Figure 1, except that the concentration of NRI∼^{32}P differed slightly from experiment to experiment. (A) Phosphatase activity of NT189 and NT169: (◇) control, (□) 1 mM ATP, (▲) 5 μM NT169, (○) 5 μM NT169 and 1 mM ATP, (×) 5 μM NT189, and (+) 5 μM NT189 and 1 mM ATP. The concentration of NRI∼P subunits was 0.14 μM. (B) Phosphatase activity of CT111 and CT126: (□) control, (▼) 1 mM AMP-PNP, (●) 3 μM CT126 and 1 mM AMP-PNP, (○) 3 μM CT126, (×) 3 μM CT111 and 1 mM AMP-PNP, (+) 3 μM CT111, (◇) 3 μM NRII, and (▲) 3 μM NRII and 1 mM AMP-PNP. The concentration of NRI∼P subunits was 0.12 μM. (C) Phosphatase activity of H-region truncations: (◇) control, (□) 1 mM ATP, (○) 5 μM MBP−H_1, (+) 5 μM MBP−H_1 and 1 mM ATP, (▲) 5 μM MBP−HX_3, (×) 5 μM MBP−HX_3 and 1 mM ATP, (▼) 5 μM MBP−HX_2, (■) 5 μM MBP−HX_2 and 1 mM ATP, (◆) 5 μM HX_3, and (△) 5 μM HX_3 and 1 mM ATP. The concentration of NRI∼P subunits was 0.14 μM. (D) PII increases the phosphatase activity of CT111 and CT126: (□) control, (○) 1 mM AMP-PNP, (+) 3 μM PII and 1 mM AMP-PNP, (△) 3 μM CT151 and 1 mM AMP-PNP, (×) 3 μM CT151, 3 μM PII, and 1 mM AMP-PNP, (▲) 3 μM CT126 and 1 mM AMP-PNP, (▼) 3 μM CT126, 3 μM PII, and 1 mM AMP-PNP, (◇) 3 μM CT111 and 1 mM AMP-PNP, and (■) 3 μM CT111, 3 μM PII, and 1 mM AMP-PNP. The concentration of NRI∼P subunits was 0.145 μM.

clearly resulted in a decreased extent of NRI phosphorylation, although not to the extent seen with the combination of NRII and PII (Figure 13B).

A direct assay for the NRII phosphatase activity involves assessing the dephosphorylation of NRI∼^{32}P, as in Figure 1. Using this assay, NT189 clearly had phosphatase activity, which was only slightly stimulated by ATP, while NT169 lacked this activity (Figure 14A). The CT111 polypeptide had detectable activity, which was reduced slightly when AMP-PNP was present (Figure 14B). This activity of CT111 was not detected in the other assays; in those assays, enhanced phosphorylation of NRI by CT111 apparently balanced the dephosphorylation of NRI∼P by CT111. Since previous studies have shown that MBP−CT111 completely lacks phosphatase activity (*18*), the observation of this activity by purified CT111 polypeptide indicates that in the fusion protein the MBP segment inhibits the phosphatase activity. The CT126 polypeptide had detectable phosphatase activity, which was inhibited by AMP-PNP (Figure 14B). While MBP−H_1 lacked discernible phosphatase activity, MBP−HX_2, MBP−HX_3, and the isolated HX_3 peptide all had phosphatase activity, which was not greatly stimulated by the presence of ATP (Figure 14C). The phosphatase activity of MBP−HX_3 and the isolated HX_3 polypeptide were nearly equal, indicating that fusion to MBP does not affect the phosphatase activity of the HX segment.

The weak phosphatase activity of CT111 and CT126 was stimulated by the PII protein (Figure 14D). Although the

stimulation of CT126 was barely detectable, stimulation of the CT111 phosphatase activity by PII was clearly discernible (Figure 14D). This result, along with the autophosphorylation data already presented, indicates that PII interacts with the NRII transmitter module.

DISCUSSION

Our studies suggest that PII activates the phosphatase activity of NRII and inhibits the autophosphorylation of NRII by stabilizing a conformation of NRII that has potent phosphatase activity. Consistent with this hypothesis, PII was not required for the phosphatase activity, and greatly activated this activity even when the cleavage of ATP by NRII was prevented (Figure 1). Furthermore, the binding of PII to NRII greatly reduced the rate of subunit exchange between NRII dimers (Figure 5), and very strongly inhibited the transphosphorylation of the central domain of NRII by NRII (Figure 11), indicating regulation of the NRII conformation by PII. Earlier studies showed that the autophosphorylation of NRII was strongly asymmetric and that PII influenced this asymmetry (*23*), suggesting that the two subunits of the NRII dimer act in a highly concerted fashion. We observed that all three domains of NRII are involved in the regulation of the NRII conformation and that all three domains of NRII are required for proper regulation of NRII activities by PII.

The most surprising result to come from our studies concerns the role of the N-terminal domain of NRII. On the basis of analogy with other two-component systems, which contain N-terminal sensory domains, it was previously thought that the N-terminal domain of NRII should serve as the site of interaction with PII. This conclusion was consistent with the observation that MBP−CT111 completely lacked phosphatase activity in the presence of PII (*18*). Indeed, the N-terminal domain of NRII is often termed the "sensory domain" (*20*, *31*). However, our experiments indicated that PII interacted with the isolated transmitter module of NRII, specifically, with the kinase domain of the transmitter module. For example, we observed that PII influenced the stoichiometry of autophosphorylation and phosphatase activity of the isolated transmitter module (Figures 10 and 14) and that PII inhibited the transphosphorylation activity of the isolated kinase domain (Figure 11). In the accompanying paper (*36*), a protein−protein cross-linking method was used to probe the interaction of PII and NRII. Consistent with our results, the results of that study show that PII interacts with the kinase domain of NRII. Thus, both the activity studies in this paper and the direct mapping of the interaction site in the accompanying paper point to the kinase domain as the site for interaction with PII.

Our studies, along with the work of Kramer and Weiss (*20*), indicate that the minimal segment of NRII required for the phosphatase activity was the central domain, consisting of the H−X region of NRII. Thus, this portion of NRII must contain the "active site" for the phosphatase activity. Yet, the phosphatase activity of this portion of NRII was weak when compared to that of the NRII−PII complex, and two constructs containing an intact transmitter module, namely, CT111 and CT126, had very weak phosphatase activity even in the presence of PII. Thus, a precise conformation of the central domain is apparently required for the phosphatase activity, and stabilization of this conformation by PII requires the presence of the N-terminal domain of NRII. Also, the interaction of the isolated central domain of NRII with NRI∼P may be poor, and in the intact protein, more extensive contacts with NRI∼P may result in more effective phosphatase activity. Finally, the phosphatase activity is likely to require the unphosphorylated form of the H-box region. This is consistent with the genetic and biochemical data indicating that mutations reducing the kinase activity of NRII increase its basal phosphatase activity (*13*, *18*). Thus, the very weak phosphatase activity of CT111 and CT126 may be due in part to the decreased asymmetry of autophosphorylation of these proteins. Interestingly, the binding of PII to CT111 and CT126 resulted in a dramatic increase in the stoichiometry of autophosphorylation of these proteins (Figure 10), and the weak phosphatase activity of these proteins in the presence of PII was only detected under conditions where their autophosphorylation was prevented (Figure 14).

The role of the N-terminal domain of NRII seems to be mainly in intramolecular signal transduction. While this domain was not required for interaction with PII, it was required for the proper response to PII binding, that is, it was required for PII to greatly stimulate the phosphatase activity and to greatly inhibit the kinase activity (both in cis and in trans). These results suggest that the N-terminal domain is involved in controlling the conformation of the central domain of NRII. The highest phosphatase activity observed among the truncated versions of NRII was that of NT189, which contains intact N-terminal and central domains. An interaction between the N-terminal domain and the central domain may be involved in stabilizing the "phosphatase" conformation of the central domain.

The N-terminal domain played a role in other activities of NRII, even in the absence of PII. For example, the N-terminal domain regulated the transphosphorylation activity of NRII, perhaps by limiting access to the NRII active site for the central domain provided in trans (Figure 8). Also, the N-terminal domain was required for highly asymmetric NRII autophosphorylation (Figure 9). In both cases, the N-terminal domain may act by limiting the flexibility of NRII. Two additional observations suggest a direct or indirect interaction between the N-terminal domain and the kinase domain. First, the N-terminal domain was required for the subunit exchange reaction, and the presence of both N-terminal domains and kinase domains was required for rapid subunit exchange. Thus, an interaction (direct or indirect) between the N-terminal and kinase domains may destabilize the NRII dimer, favoring subunit exchange. Second, an unfavorable interaction between the N-terminal and kinase domains appears to contribute to the instability of the doubly phosphorylated NRII dimer, since doubly phosphorylated NT189 dimers appeared to be unusually stable (Figure 7 and data not shown). One possible explanation for these results is that the two N-terminal domains of NRII interact with the central and kinase domains in the dimer. The N-terminal domain of NRII contains a PAS motif, which in certain other proteins is thought to mediate interactions between domains (*37*; for a review, see ref *38*).

How does PII bring about the phosphatase activity of NRII? An admittedly speculative model that is nevertheless consistent with the existing genetic and biochemical data is

as follows. We hypothesize that the phosphorylation of NRI by NRII may proceed by an alternating-sites mechanism, in which the hemiphosphorylated NRII dimer must transfer its phosphoryl group to NRI before the second subunit of NRII can become phosphorylated. Yet, existing data suggest that in the hemiphosphorylated state, the autophosphorylation of the second subunit is occurring rapidly, but its dephosphorylation is occurring more rapidly (*23*). Thus, we imagine that in hemiphosphorylated NRII, the unphosphorylated subunit is in close association with the kinase domain of the other subunit. Upon dephosphorylation of hemiphosphorylated NRII by NRI, the previously unphosphorylated NRII subunit rapidly becomes phosphorylated and NRII undergoes a conformational change in which the two subunits trade conformations. That is, the phosphorylated subunit is moved into position for interaction with NRI, and the unphosphorylated subunit is moved out of position for interaction with NRI and into close association with the opposing kinase domain. Thus, the unphosphorylated H-box region of NRII is seldom in position to interact with NRI∼P, explaining the low phosphatase activity of NRII in the absence of PII. PII may act by slowing the alternating-sites cycle after dephosphorylation of NRII∼P by NRI. This would cause the unphosphorylated H-box region of NRII to persist in a conformation that is ideal for interaction with NRI∼P. However, PII also seems to act in a positive sense to force NRII into the conformation that displays phosphatase activity (Figure 1). Thus, we hypothesize that PII both slows the alternating-sites phosphorylation mechanism and forces the unphosphorylated H-box region into the conformation displaying phosphatase activity. Since the binding of PII to NRII inhibited the subunit exchange reaction, PII apparently stabilizes the dimer in this phosphatase conformation. Of course, other models may be envisioned, and future work must address the issue of whether the kinase reaction proceeds by an alternating-sites mechanism.

We used transphosphorylation assays to examine the activity of various constructs derived from NRII. Our results suggest that transphosphorylation may have occurred by distinct mechanisms in these experiments, depending on the kinase−substrate pair. Phosphorylation of substrates by CT190, which lacks any ability to form heterodimers owing to no overlap with the substrates, probably represents a true intermolecular phosphorylation. Phosphorylation of NT189 by wild-type NRII, on the other hand, may occur primarily in heterodimers, since NT189 and NRII readily form heterodimers. We did not detect any ability of CT111, CT126, NT169, MBP−HX_2, MBP−HX_3, or the isolated HX_3 polypeptide to form heterodimers using our gel electrophoresis assay; however, the possibility remains that these polypeptides may form heterodimers that are very unstable. Thus, for these, we cannot exclude the possibility that some of the transphosphorylation phenomena were due to intramolecular reactions in heterodimers.

Dimerization and Domain Organization of NRII. Our studies on the domain organization and dimerization of NRII were generally consistent with structural studies of Spo0B, EnvZ, and CheA, as well as previous functional dissections of these proteins and NRII. These studies indicate that the transmitter module is actually two domains and that the main dimerization determinants are within the N-termini of these, which form a four-helix bundle in the dimer. We observed that this segment of NRII, when grafted onto the monomeric MBP, brought about dimerization of MBP. However, our studies of subunit exchange showed that the stability of the NRII dimer is affected by the other domains of the protein.

The X-box region of NRII was not required for dimerization per se. For example, NT125, NT135, NT145, NT155, and NT169 were dimers as purified after overexpression. Indeed, NT125 completely lacks both H- and X-motifs, yet was dimeric. However, NT110 was clearly monomeric. Therefore, a segment of NRII mapping between positions 110 and 125 seems to be involved in dimerization of these polypeptides. This region of NRII is thought to be a linker region connecting the N-terminal domain and the transmitter module. The dimerization of these NT polypeptides may reflect an unnatural process not observed with native NRII. NT125, NT135, NT145, NT155, and NT169 did not undergo subunit exchange with NRII or MBP−NRII. One possibility is that in the absence of the intact H−X region, the segment of NRII between positions 110 and 125 may be in an unnatural conformation. This conclusion is consistent with our observation that NT145 and NT155 could not be phosphorylated by wild-type NRII and that NT169 could be efficiently phosphorylated only by wild-type NRII, despite the fact that NT145, NT155, and NT169 contain the H-box region. Also, the slow rate of NT169∼P dephosphorylation by NRI suggested that this species is in an unnatural conformation.

The CT series of proteins provides information about dimerization determinants in the transmitter domain of NRII. CT111 and CT126 were dimers, while CT190 was a monomer. CT151 behaved as if it formed very unstable dimers. MBP−CT111 and MBP−CT126 were also mostly dimeric, while MBP−CT151 was mostly monomeric. These results suggest that positions 126−190, that is, the H−X region, were involved in dimerization and that positions 151−190, that is, the X region, had weak dimerization potential by itself.

Previous results have shown that mutations in the X-box region may result in a reduced ability to negatively regulate system output in vivo, which has been interpreted as signifying a decrease in the phosphatase activity (*13*, *17*). Since our results show that the X-box is involved in dimerization and subunit exchange, one possibility is that the X-box mutations alter the conformation in a way that favors phosphorylation of the H-box under conditions where it typically is not phosphorylated. For example, these mutations may affect the phosphatase activity by diminishing the asymmetry of NRII autophosphorylation. Alternatively, these mutations in the central domain may destabilize the conformation with high phosphatase activity.

ACKNOWLEDGMENT

We thank members of our laboratory for helpful comments on the manuscript and our colleagues Augen Pioszak, Emmanuel S. Kamberov, and Phyllis Zucker for contributing some of the purified proteins used in these studies.

REFERENCES

1. Ninfa, A. (1996) Regulation of gene transcription by extracellular stimuli, in *Escherichia coli and Salmonella: Cellular and Molecular Biology* (Neidhardt, F. C., Ed.) 2nd ed., pp 1246−1262, American Society for Microbiology, Washington, DC.

2. Weiss, V., and Magasanik, B. (1988) *Proc. Natl. Acad. Sci. U.S.A. 85*, 8919−8923.
3. Ninfa, A. J., and Bennett, R. L. (1991) *J. Biol. Chem. 266*, 6888−6893.
4. Hess, J. F., Oosawa, N., Kaplan, N., and Simon, M. I. (1988) *Cell 53*, 79−87.
5. Sanders, D. A., Gillece-Castro, B. L., Burlingame, A. L., and Koshland, D. E., Jr. (1992) *J. Bacteriol. 174*, 5117−5122.
6. Burbulys, D., Trach, K. A., and Hoch, J. A. (1991) *Cell 64*, 545−552.
7. Ninfa, A. J., and Magasanik, B. (1986) *Proc. Natl. Acad. Sci. U.S.A. 83*, 5909−5913.
8. Keener, J., and Kustu, S. (1988) *Proc. Natl. Acad. Sci. U.S.A. 85*, 4976−4980.
9. Popov, K. M., Zhao, Y., Shinmomura, Y., Kuntz, M. J., and Harris, R. A. (1992) *J. Biol. Chem. 267*, 13127−13130.
10. Park, H., Saha, S. K., and Inouye, M. (1998) *Proc. Natl. Acad. Sci. U.S.A. 95*, 6728−6732.
11. Tanaka, T., Saha, S. K., Tomomori, C., Ishima, R., Liu, D., Tong, K. I., Park, H., Dutta, R., Qin, L., Swindells, M. B., Yamazaki, T., Ono, A. M., Kainosho, M., Inouye, M., and Ikura, M. (1998) *Nature 396*, 88−92.
12. Bilwes, A. M., Alex, L. A., Crane, B. R., and Simon, M. I. (1999) *Cell 96*, 131−141.
13. Atkinson, M. R., and Ninfa, A. J. (1993) *J. Bacteriol. 175*, 7016−7023.
14. Varughese, K. I., Madhusudan, Zhou, X. Z., Whiteley, J. M., and Hoch, J. A. (1998) *Mol. Cell 2*, 485−493.
15. Chou, K., Maggiora, G. M., Nemethy, G., and Scheraga, H. A. (1988) *Proc. Natl. Acad. Sci. U.S.A. 85*, 4295−4299.
16. Tomomori, C., Tanaka, T., Dutta, R., Park, H., Saha, S. K., Zhu, Y., Ishima, R., Liu, D., Tong, K. I., Kurokawa, H., Qian, H., Inouye, M., and Ikura, M. (1999) *Nat. Struct. Biol. 6*, 729−734.
17. Hsing, W., Russo, F. D., Bernd, K. K., and Silhavy, T. J. (1998) *J. Bacteriol. 180*, 4538−4546.
18. Kamberov, E. S., Atkinson, M. R., Chandran, P., and Ninfa, A. J. (1994) *J. Biol. Chem. 269*, 28294−28299.
19. Swanson, R. V., Schuster, S. C., and Simon, M. I. (1993) *Biochemistry 32*, 7623−7629.
20. Kramer, G., and Weiss, V. (1999) *Proc. Natl. Acad. Sci. U.S.A. 96*, 604−609.
21. Yang, Y., and Inouye, M. (1991) *Proc. Natl. Acad. Sci. U.S.A. 88*, 11057−11061.
22. Ninfa, E. G., Atkinson, M. R., Kamberov, E. S., and Ninfa, A. J. (1993) *J. Bacteriol. 175*, 7024−7032.
23. Jiang, P., Peliska, J. A., and Ninfa, A. J. (2000) *Biochemistry 39*, 5057−5065.
24. Jiang, P., and Ninfa, A. J. (1999) *J. Bacteriol. 181*, 1906−1911.
25. Atkinson, M. R., and Ninfa, A. J. (1992) *J. Bacteriol. 174*, 4538−4548.
26. Kamberov, E. S., Atkinson, M. R., Feng, J., Chandran, P., and Ninfa, A. J. (1994) *Cell. Mol. Biol. Res. 40*, 175−191.
27. Jiang, P., Peliska, J. A., and Ninfa, A. J. (1998) *Biochemistry 37*, 12782−12794.
28. Jiang, P., Zucker, P., Atkinson, M. R., Kamberov, E. S., Tirasophon, W., Chandran, P., Schefke, B. R., and Ninfa, A. J. (1997) *J. Bacteriol. 179*, 4342−4353.
29. Schauder, B., Blocker, H., Frank, R., and McCarthy, J. E. G. (1987) *Gene 52*, 279−283.
30. Bueno, R., Pahel, G., and Magasanik, B. (1985) *J. Bacteriol. 164*, 816−822.
31. Silhavy, T. J., Berman, M. L., and Enquist, L. W. (1984) *Experiments with gene fusions*, pp 107−111, Cold Spring Harbor Laboratory Press, Cold Spring Harbor, NY.
32. Ueno-Nishio, S., Mango, S., Reitzer, L. J., and Magasanik, B. (1984) *J. Bacteriol. 160*, 379−384.
33. Feng, J., Atkinson, M. R., McCleary, W., Stock, J. B., Wanner, B. L., and Ninfa, A. J. (1992) *J. Bacteriol. 174*, 6061−6070.
34. Ninfa, A. J., Ueno-Nishio, S., Hunt, T. P., Robustell, B., and Magasanik, B. (1986) *J. Bacteriol. 168*, 1002−1004.
35. Kamberov, E. S., Atkinson, M. R., and Ninfa, A. J. (1995) *J. Biol. Chem. 270*, 17797−17807.
36. Pioszak, A., Jiang, P., and Ninfa, A. J. (2000) *Biochemistry 39*, 13450−13461.
37. Takahata, S., Sogawa, K., Kobayashi, A., Ema, M., Mimura, J., Ozaki, N., and Fujii-Kuriyama, Y. (1998) *Biochem. Biophys. Res. Commun. 248*, 789−794.
38. Ponting, C. P., and Aravind, L. (1997) *Curr. Biol. 7*, R674−R677.

BI000794U